







# ArfGAP1 inhibits mTORC1 lysosomal localization and activation

Delong Meng<sup>1,2,3</sup> , Qianmei Yang<sup>1,2,3</sup>, Chase H Melick<sup>1,2,3</sup> , Brenden C Park<sup>1,2,3</sup>, Ting-Sung Hsieh<sup>1,2,3</sup> , Adna Curukovic<sup>1,2,3</sup>, Mi-Hyeon Jeong<sup>1,2,3</sup>, Junmei Zhang<sup>1</sup> , Nicholas G James<sup>4</sup>  & Jenna L Jewell<sup>1,2,3,\*</sup> 

## Abstract

The mammalian target of rapamycin complex 1 (mTORC1) integrates nutrients, growth factors, stress, and energy status to regulate cell growth and metabolism. Amino acids promote mTORC1 lysosomal localization and subsequent activation. However, the subcellular location or interacting proteins of mTORC1 under amino acid-deficient conditions is not completely understood. Here, we identify ADP-ribosylation factor GTPase-activating protein 1 (ArfGAP1) as a crucial regulator of mTORC1. ArfGAP1 interacts with mTORC1 in the absence of amino acids and inhibits mTORC1 lysosomal localization and activation. Mechanistically, the membrane curvature-sensing amphipathic lipid packing sensor (ALPS) motifs that bind to vesicle membranes are crucial for ArfGAP1 to interact with and regulate mTORC1 activity. Importantly, ArfGAP1 represses cell growth through mTORC1 and is an independent prognostic factor for the overall survival of pancreatic cancer patients. Our study identifies ArfGAP1 as a critical regulator of mTORC1 that functions by preventing the lysosomal transport and activation of mTORC1, with potential for cancer therapeutics.

**Keywords** amino acids; ArfGAP1; lysosome; mTORC1; vesicle trafficking

**Subject Categories** Membranes & Trafficking; Metabolism

**DOI** 10.15252/emboj.2020106412 | Received 3 August 2020 | Revised 14 March 2021 | Accepted 24 March 2021 | Published online 14 May 2021

**The EMBO Journal (2021) 40: e106412**

## Introduction

Multiple stimuli like amino acids, stress, growth factors, and energy status regulate mTORC1 activity in order to control cell growth and metabolism (Ben-Sahra & Manning, 2017; Gonzalez & Hall, 2017; Meng *et al.*, 2018). Importantly, hyperactivation of mTORC1 is often involved in many human diseases like cancer, obesity, type 2 diabetes, and neurodegeneration (Blenis, 2017; Liu & Sabatini, 2020). When amino acids are limiting, mTORC1 is inactive and dispersed throughout the cell at an unknown location. In contrast, elevated amino acids increase mTORC1 lysosomal localization and

subsequent activation (Kim *et al.*, 2008; Sancak *et al.*, 2008). mTORC1 is then activated downstream of growth factor signaling by the lysosomal localized small GTPase Ras homolog enriched in brain (Rheb) (Inoki *et al.*, 2003; Tee *et al.*, 2003; Zhang *et al.*, 2003; Yang *et al.*, 2017). The last 15 amino acids with a CAAX (C = cysteine, A = aliphatic, X = terminal amino acid) motif at the C-terminus of Rheb anchors it to the lysosome (Sancak *et al.*, 2010; Menon *et al.*, 2014; Yang *et al.*, 2017).

Different amino acids can activate mTORC1 through distinct signaling cascades and mechanisms. For example, leucine (Leu), arginine (Arg), methionine (Met), and some other amino acids activate mTORC1 through the well-characterized Rag GTPase pathway to mTORC1 (Hara *et al.*, 1998; Kim *et al.*, 2008; Sancak *et al.*, 2008; Bauchart-Thevret *et al.*, 2010; Zoncu *et al.*, 2011; Chantranupong *et al.*, 2016; Wolfson *et al.*, 2016; Gu *et al.*, 2017; Meng *et al.*, 2020). Four Rag genes are in mammals (Kim *et al.*, 2008; Sancak *et al.*, 2008). RagA and RagB are high in sequence similarity and functionally redundant, whereas RagC and RagD are also highly related in sequence and functionally redundant. RagA or RagB can form a heterodimer with RagC or RagD, which is important for mTORC1 activation and the protein stability of the Rag GTPases (Jewell *et al.*, 2015). RagA or RagB GTP-bound can interact with Raptor (mTORC1 component) at the lysosome. In contrast, RagC or RagD GDP-bound forms a heterodimer with the GTP-bound RagA or RagB. Rag GTPase guanine nucleotide loading is controlled by guanine nucleotide exchange factors (GEFs) and GTPase-activating proteins (GAPs). A pentameric complex called the Ragulator and the amino acid transporter solute carrier family 38 member 9 (SLC38A9) have been shown to act as GEFs for RagA or RagB (Sancak *et al.*, 2008; Sancak *et al.*, 2010; Bar-Peled *et al.*, 2012). GATOR1 acts as a GAP for RagA or RagB (Bar-Peled *et al.*, 2013), whereas folliculin is a GAP for RagC or RagD (Tsun *et al.*, 2013). In addition, glutamine (Gln) and asparagine (Asn) activate mTORC1 in a Rag GTPase-independent manner and require the small GTPase ADP-ribosylation factor 1 (Arf1) (Jewell *et al.*, 2015; Meng *et al.*, 2020). The guanine nucleotide cycling of Arf1 is important in the regulation of mTORC1 by Gln and Asn. However, the mechanistic details are still unclear. The GEFs and GAPs involved in this pathway have yet to be identified. Thus, amino acids activate mTORC1 through two distinct pathways.

1 Department of Molecular Biology, University of Texas Southwestern Medical Center, Dallas, TX, USA

2 Harold C. Simmons Comprehensive Cancer Center, University of Texas Southwestern Medical Center, Dallas, TX, USA

3 Hamon Center for Regenerative Science and Medicine, University of Texas Southwestern Medical Center, Dallas, TX, USA

4 Department of Cell and Molecular Biology, John A. Burns School of Medicine, University of Hawaii, Honolulu, HI, USA

\*Corresponding author. Tel: +1 214 648 1086; E-mail: jenna.jewell@utsouthwestern.edu

The subcellular localization is critical for regulating mTORC1 activity (Sancak *et al*, 2010; Efeyan *et al*, 2012; Betz & Hall, 2013; Terenzio *et al*, 2018). However, it has been a long-standing question of where mTORC1 is when it is not at the lysosome and how mTORC1 is trafficked throughout the cell (Betz & Hall, 2013; Lawrence & Zoncu, 2019). Intracellular trafficking is tightly regulated by a variety of proteins, with small GTPases being critical players involved in this process (Itzen & Goody, 2011). Multiple small GTPases like Rheb, Rags, Rab1A, Rab5, RalA, Rac1, and Arf1 have been shown to alter mTORC1 lysosomal localization and activity (Duran & Hall, 2012; Nguyen *et al*, 2017; Zhu & Wang, 2020). For example, the Rag GTPases sense multiple amino acids and directly bind to Raptor, anchoring mTORC1 to the lysosomal surface (Kim *et al*, 2008; Sancak *et al*, 2008; Sancak *et al*, 2010). Rab1A was shown to interact with mTORC1, promoting amino acid-induced mTORC1 activity at the Golgi (Thomas *et al*, 2014). Rab5 disruption leads to mTORC1 retention on mixed early and late endosomes regardless of amino acid availability (Flinn *et al*, 2010; Li *et al*, 2010). RalA regulates mTORC1 through modulating the activity of phospholipase D in response to nutrients (Maehama *et al*, 2008; Xu *et al*, 2011). Rac1 interacts with mTORC1 and regulates its subcellular localization (Saci *et al*, 2011). Arf1 is required for Gln and Asn signaling to mTORC1 (Jewell *et al*, 2015; Meng *et al*, 2020). Small GTPases cycle between an active GTP-bound and inactive GDP-bound conformation (Bos *et al*, 2007). GEFs activate G proteins by promoting the exchange of GDP to GTP, whereas GAPs act antagonistically to deactivate G proteins by increasing their intrinsic rate of GTP hydrolysis. It is worth noting that the role of GEFs and GAPs are not solely “activators” or “inactivators” switches for small G proteins. For example, GEFs and GAPs can also act as a scaffold or effector in signaling transduction and cellular processes, extending their potential roles in regulating cell signaling pathways (Donaldson & Jackson, 2011). However, it is still not completely clear how mTORC1 localization and activity are controlled by small GTPases and their regulators.

To further understand the molecular mechanisms by which mTORC1 is trafficked to the lysosome and activated, we investigated the role of ArfGAP1 in mTORC1 regulation. Under amino acid starvation conditions, ArfGAP1 binds to mTORC1 sequestering mTORC1 away from the lysosome and preventing mTORC1 activation. The

membrane curvature-sensing amphipathic lipid packing sensor (APLS) motifs of ArfGAP1 are critical for mTORC1 activation. Furthermore, ArfGAP1 plays a key role in mTORC1-mediated biology and the overall survival of pancreatic cancer patients.

## Results

### ArfGAP1 interacts with mTORC1

To identify potential mTORC1-interacting proteins, we immunopurified the mTORC1 complex from cells using Flag-tagged Raptor. Mass spectrometry analysis of anti-Flag immunoprecipitates identified ArfGAP1 as a potential interacting partner of mTORC1. We confirmed that HA-tagged ArfGAP1 interacted with endogenous mTORC1 by immunoprecipitation experiments in HEK293A cells (Fig 1A). Moreover, immunoprecipitation of an endogenously C-terminal GFP-tagged Raptor from the near-haploid HAP1 cell line (Manifava *et al*, 2016) revealed an endogenous interaction between ArfGAP1 and mTORC1 (Fig 1B). Thus, ArfGAP1 interacts with mTORC1 in different cell lines.

Amino acids promote lysosomal localization and activation of mTORC1 in Rag GTPase-dependent (Kim *et al*, 2008; Sancak *et al*, 2008; Sancak *et al*, 2010) and independent manner (Jewell *et al*, 2015; Meng *et al*, 2020). Because the Rag GTPases can directly interact with mTORC1 via Raptor and anchor mTORC1 to the lysosome (Sancak *et al*, 2008), we investigated whether the ArfGAP1-mTORC1 interaction is dependent on the Rag GTPases. Utilizing either wild-type or RagA/B GTPase knockout (KO) HEK293A cells that were previously described (Jewell *et al*, 2015), Flag-tagged Raptor or HA-tagged ArfGAP1 were overexpressed and immunoprecipitates were analyzed (Fig 1C–E). There are four Rag GTPases in mammals: RagA, RagB, RagC, and RagD (Kim *et al*, 2008; Sancak *et al*, 2008). RagA/B KO cells have depleted levels of RagC/RagD, because RagC/RagD protein levels are stabilized by RagA/B-RagC/D heterodimerization. Thus, RagA/B KO cells do not have intact Rag GTPase complexes (Jewell *et al*, 2015). Interestingly, ArfGAP1 can still confer interaction with mTORC1 in the absence of the Rag GTPases. ArfGAP1 was the first Arf GAP that was cloned

#### Figure 1. ArfGAP1 and mTORC1 interact in cells.

- Human embryonic kidney 293A (HEK293A) cells were transfected with HA-tagged ArfGAP1 or HA-tagged RFP1 as a control for 24 h. Cell lysates were immunoprecipitated with anti-HA beads. Immunoprecipitates (IP) or whole cell lysate (WCL) samples were probed for HA and the mTORC1 components (mTOR, Raptor, and mLST8). Vinculin was probed as a control.
- Wild-type (Ctrl) or Raptor endogenously GFP-tagged (Raptor-GFP) HAP1 cells were immunoprecipitated with GFP antibody and protein A/G beads. IP or WCL samples were probed for GFP and ArfGAP1.
- Flag-tagged Raptor was transfected with HA-tagged ArfGAP1 or HA-tagged RFP1 in wild-type (WT) or RagA/B knockout (KO) HEK293A cells for 24 h. Cell lysates were immunoprecipitated with anti-Flag beads. IP or WCL samples were probed for HA-tagged ArfGAP1 or HA-tagged RFP1, Flag-tagged Raptor, RagA, RagB, and Vinculin the loading control.
- RagA/B KO HEK293A cells (control or stably overexpressing Flag-tagged Raptor) were transfected with HA-tagged ArfGAP1 or empty vector for 24 h. Cell lysates were immunoprecipitated with anti-Flag or anti-HA beads as indicated. IP or WCL samples were probed for HA-tagged ArfGAP1, Flag-tagged Raptor, and other mTORC1 components mTOR and mLST8.
- HEK293A cells were transfected with empty vector (EV) or Flag-tagged Raptor with or without HA-tagged ArfGAP1 for 24 h. Cell lysates were immunoprecipitated with anti-Flag beads. IP and WCL samples were probed for Flag-tagged Raptor, HA-tagged ArfGAP1, mTOR, and the phosphorylation of mTOR at Serine 2481.
- Schematic of distribution and comparison of domains between human ArfGAP1, ArfGAP2, and ArfGAP3 proteins.
- RagA/B KO HEK293A cells were transfected with HA-tagged ArfGAP1, HA-tagged ArfGAP2, or HA-tagged RFP1 (control) for 72 h. Cell lysates were immunoprecipitated with anti-HA beads. IP or WCL samples were probed for HA and mTORC1 components mTOR, Raptor, and mLST8. Vinculin was probed as a control.

Source data are available online for this figure.

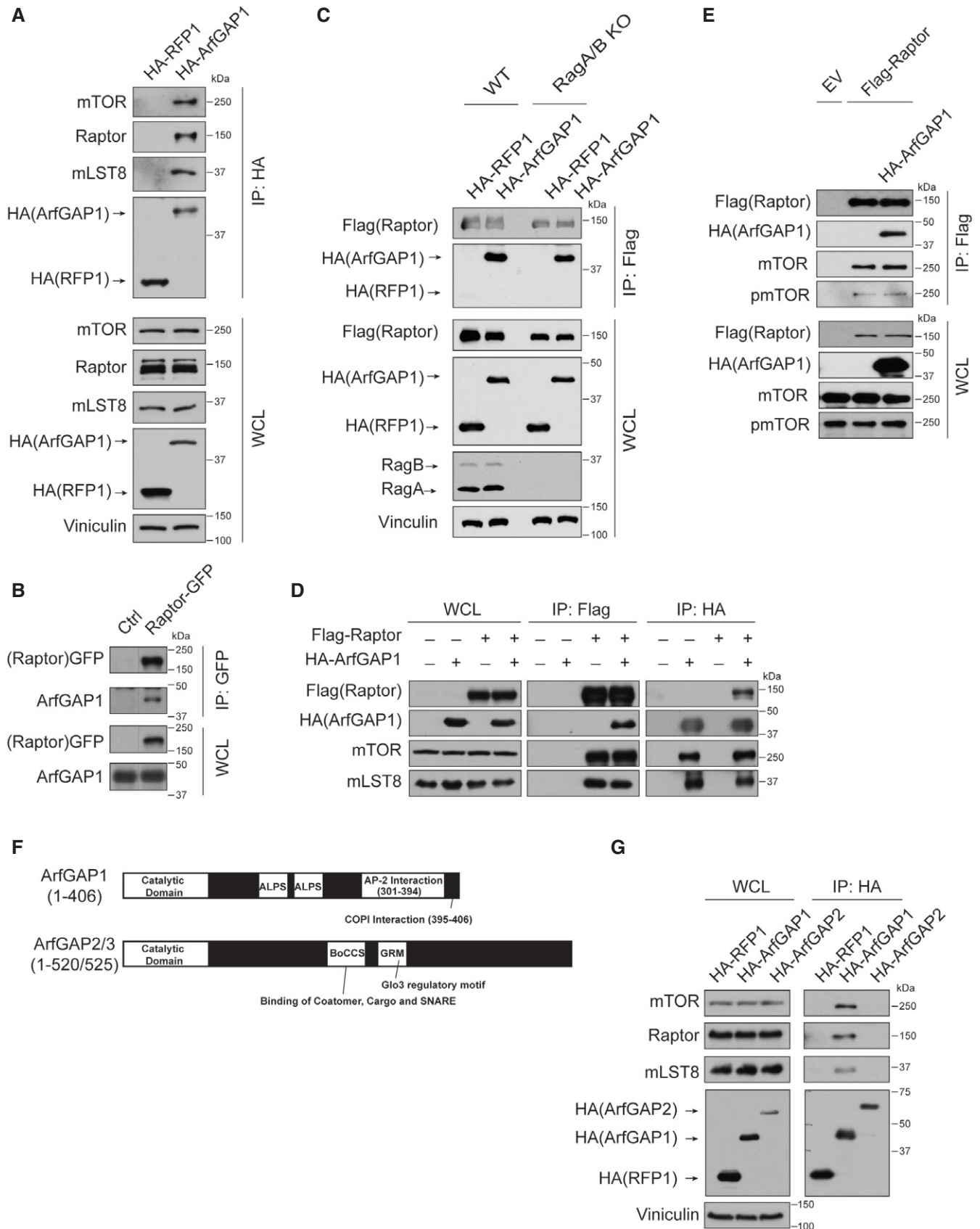


Figure 1.

(Cukierman *et al*, 1995; Makler *et al*, 1995) and has to date been reported to target and act as a GAP for Arfs 1-5 (Donaldson & Jackson, 2011) and leucine-rich repeat kinase 2 (LRRK2) (Stafa *et al*, 2012; Xiong *et al*, 2012). There are more than 30 human Arf GAPs, with ArfGAP2 and ArfGAP3 having the highest sequence similarity (~30%) to ArfGAP1 (Fig 1F) (Spang *et al*, 2010). However, co-immunoprecipitation of HA-tagged ArfGAP2 was unable to interact with mTORC1, revealing specificity of ArfGAP1 binding to mTORC1 (Fig 1G). Thus, ArfGAP1, but not ArfGAP2, binds to mTORC1 and this interaction is not dependent on the Rag GTPases.

### ArfGAP1 inhibits mTORC1 activation

Some amino acids activate mTORC1 through the Rag GTPase pathway (Fig 2A left, Appendix Fig S1A and B) (Chantranupong *et al*, 2016; Wolfson *et al*, 2016; Gu *et al*, 2017). In contrast, our laboratory has established that Gln and Asn activate mTORC1 through a Rag GTPase-independent pathway that requires Arf1 (Fig 2A right, Appendix Fig S1C) (Jewell *et al*, 2015; Meng *et al*, 2020). mTORC1 activity is analyzed by the phosphorylation of the well-characterized mTORC1 substrates S6K1, 4EBP1, ULK1, and the S6K1 substrate S6. The phosphorylation of S6K1 and 4EBP1 promotes protein translation, whereas the phosphorylation of ULK1 inhibits autophagy (Burnett *et al*, 1998; Kim *et al*, 2011; Jewell *et al*, 2013; Ben-Sahra & Manning, 2017). ArfGAP1 has been shown to be a GAP for Arf1

(Donaldson & Jackson, 2011), and we previously reported that the guanine nucleotide cycling of Arf1 is involved in Gln and Asn signaling to mTORC1 (Jewell *et al*, 2015; Meng *et al*, 2020). However, the mechanistic details of how Arf1 regulates mTORC1 are currently unknown. Because both the guanine nucleotide cycling of Arf1 (Arf1 GTP-bound and Arf1 GDP-bound) and ArfGAP1 regulate Gln and Asn signaling to mTORC1, it is possible that ArfGAP1 is involved in this process. However, overexpression of Arf1, Arf1 GTP-bound, Arf1 GDP-bound, or a fast-cycling Arf1 mutant (Arf1 T161A) could not alter mTORC1 inhibition by ArfGAP1 (Appendix Fig S2A and B). Moreover, treatment with Brefeldin A (BFA, an Arf1 GEF inhibitor) does not alter the mTORC1-ArfGAP1 complex, suggesting that the Arf1 activity is not involved in the ArfGAP1-mTORC1 interaction (Appendix Fig S2C).

Because ArfGAP1 interacts with mTORC1, we tested if ArfGAP1 played a role in mTORC1 activation. HA-tagged ArfGAP1 and either Myc-tagged S6K1 (Fig 2B and C) or Myc-tagged 4EBP1 (EV1A) were overexpressed in HEK293A cells. Cells were starved of amino acids, stimulated with different amino acids (Rag-dependent Leu, or Rag-independent Gln and Asn), and Myc-tagged immunoprecipitates were analyzed. Interestingly, overexpression of ArfGAP1 inhibited amino acid-induced mTORC1 activation (Figs 2B and C, and EV1A and B). Consistently, knocking down ArfGAP1 using short hairpin RNAs (shRNAs) enhanced mTORC1 activation by Leu, Met, Arg, Gln, and Asn (Figs 2D and EV1C and D). Following depletion of

**Figure 2. ArfGAP1 regulates mTORC1 signaling.**

- A Model of Rag GTPase-dependent and Rag GTPase-independent pathways that signal to mTORC1. Alanine (Ala), arginine (Arg), histidine (His), leucine (Leu), methionine (Met), serine (Ser), threonine (Thr), and valine (Val) promote mTORC1 lysosomal localization and activation through the Rag GTPase pathway. Glutamine (Gln) and asparagine (Asn) promote mTORC1 lysosomal localization and activation independently of the Rag GTPases and require Arf1 through an unknown mechanism. Both pathways require growth factor signaling resulting in Rheb GTP-bound allosterically activating mTORC1.
- B Human embryonic kidney 293A (HEK293A) cells were co-transfected with HA-tagged ArfGAP1 or HA-tagged RFP1 (control), together with Myc-tagged S6K1. Cells were starved of amino acids for 1 h (–AA), and then, 1 mM of leucine (+Leu), glutamine (+Gln), or asparagine (+Asn) was added for 2 h. Immunoprecipitates (IP) or whole cell lysate (WCL) samples were probed for HA, Myc, and phosphorylated S6K1 at Thr 389 (pS6K1). Vinculin was a loading control.
- C Wild-type (WT) or RagA/B knockout (KO) HEK293A cells were co-transfected with HA-tagged ArfGAP1 or HA-tagged RFP1 (control) with Myc-tagged S6K1. Cells were starved of amino acids (–AA) for 2 h, and then, 4 mM of glutamine (+Gln) or asparagine (+Asn) was added for 2 h. Cell lysates were assessed for mTORC1 activity by the phosphorylation of S6K1 at Thr 389 (pS6K1) and probed for HA, Myc, S6K1, RagA, RagB, and Vinculin.
- D ArfGAP1 was stably knocked down in HEK293A cells using shRNAs against ArfGAP1 (shArfGAP1) or GFP (shGFP) control. Cells were cultured under normal condition (NC; lanes 1 and 8) or starved of amino acids for 1 h (–AA 1h; lanes 2 and 9), followed by either maintaining in amino acid starvation media (–AA; lanes 3 and 10), or addition of 1 mM of Leu (+Leu; lanes 4 and 11), Gln (+Gln; lanes 5 and 12), or Asn (+Asn; lanes 6 and 13) for 2 h. mTORC1 activity was analyzed similar to (C). Protein levels of ArfGAP1 were confirmed by immunoblotting. S6K1 and actin were probed as controls.
- E RagA/B KO HEK293A cells were co-transfected with HA-tagged ArfGAP1, HA-tagged ArfGAP2, or HA-tagged RFP1 (control) with Myc-tagged S6K1. Cells were starved of amino acids (–AA) for 2 h, and then, 4 mM of Gln or Asn was added for 2 h. mTORC1 was analyzed similar to (B). IP or WCL samples were probed for HA, Myc, and phosphorylated S6K1 at Thr 389 (pS6K1). Actin serve as a loading control.
- F RagA/B KO HEK293A cells were transfected with HA-tagged ArfGAP1 for 24 h. Immunofluorescence assay was performed to stain HA-tagged ArfGAP1 (green) and pS6 at Serine 235/236 (red). A representative image of the staining of two channels is shown (scale bar, 20  $\mu$ m). 8 fields were randomly chosen for quantification analysis, and total cell numbers are summarized in the table (Fisher's exact test  $P < 0.0001$ ). Percentages of pS6-positive cells in each field for HA-tagged ArfGAP1-positive or ArfGAP1-negative cell populations are illustrated in the bar plot (shown as Mean  $\pm$  SEM; Student's  $t$ -test  $P = 2.1 \times 10^{-6}$ ).
- G ArfGAP1 was knocked out using CRISPR/Cas9 in RagA/B KO HEK293A cells. Expression levels of ArfGAP1 in two KO clones (KO-1 and KO-2) were confirmed by immunoblotting, and mTORC1 activity was analyzed as in (C).
- H RagA/B KO HEK293A or RagA/B KO ArfGAP1 KO HEK293A cells were starved of amino acids (–AA) for 2 h and stimulated with 4 mM Gln (+Gln) or Asn (+Asn) for 2 h. Lysates were analyzed for mTORC1 activity as in (C), and phosphorylation of S6 at Serine 235/236 (pS6) was also analyzed. ArfGAP1 and Actin were probed for as controls.
- I RagA/B KO HEK293A or RagA/B KO ArfGAP1 KO HEK293A cells were starved of amino acids for 1, 2, and 4 h. NC denotes normal condition. Lysates were analyzed as in (H). "s.e." and "l.e." denote short exposure and long exposure, respectively.
- J RagA/B KO HEK293A cells (lanes 1, 2), RagA/B KO ArfGAP1 KO HEK293A cells (KO-1) (lanes 3, 4), RagA/B KO ArfGAP1 KO HEK293A cells with HA-tagged ArfGAP1 overexpressed for 24 h (lanes 5, 6) were cultured under normal condition (NC) or starved of amino acids (–AA) for 30 min. mTORC1 activity was analyzed as in (H).
- K WT HEK293A cells were co-transfected with HA-tagged ArfGAP1 or HA-tagged RFP1 (control) with Myc-tagged S6K1. Cells were cultured under normal condition (NC), or starved of serum (–Serum) for overnight and then treated with 100 nM insulin (+Insulin) for 30 min. mTORC1 activity was assessed similar to (C). Cell lysates were probed for HA, S6K1, phosphorylated S6K1 at threonine 389 (pS6K1), mTOR, phosphorylated mTOR at Serine 2481 (pmTOR), and Vinculin.

Source data are available online for this figure.

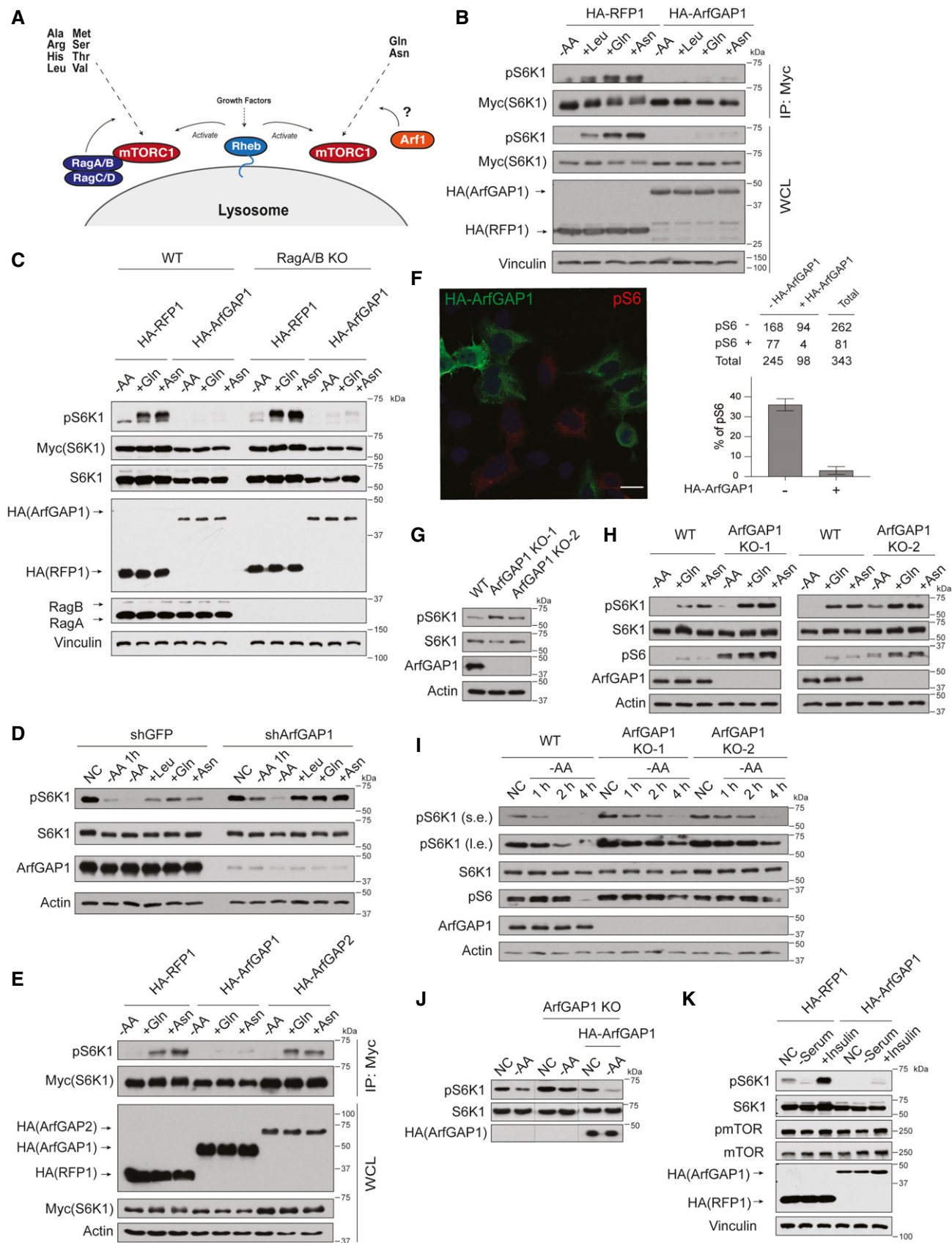


Figure 2.



ArfGAP1, mTORC1 activity is less sensitive to amino acid starvation (Fig 2D; lane 2 versus lane 9). These results suggest that ArfGAP1 inhibits mTORC1 activity. Moreover, not only did ArfGAP2 not interact with mTORC1 (Fig 1G), overexpression of ArfGAP2 did not alter mTORC1 activation by amino acids (Figs 2E and EV1A). mTORC1 activity can also be assessed by immunofluorescence staining of phosphorylated S6, a S6K1 substrate (Jewell *et al.*, 2015). Overexpression of HA-tagged ArfGAP1 (green) in cells revealed no phosphorylation of S6 (pS6) staining (red), whereas cells with high pS6 did not have HA-tagged ArfGAP1 expressed (Fig 2F). Taken together, ArfGAP1 regulates the activity of mTORC1.

To further investigate the role of ArfGAP1 in respect to mTORC1 activation, we utilized CRISPR/Cas9 technology and generated two different clones of ArfGAP1 KO HEK293A cells. ArfGAP1 KO cells were confirmed by immunoblotting (Fig 2G) and genomic DNA sequencing (EV1E). Similar to the experiments where ArfGAP1 was depleted by shRNA (Figs 2D and EV1D), amino acids enhanced mTORC1 activity, and mTORC1 was resistant to amino acid withdrawal in ArfGAP1 KO cells (Fig 2H and I). Put-back experiments were performed re-introducing HA-tagged ArfGAP1 in ArfGAP1 KO cells. Overexpression of HA-tagged ArfGAP1 in ArfGAP1 KO cells decreased mTORC1 to similar levels as wild-type cells upon the removal of amino acids (Fig 2J). As expected, similar to overexpression of ArfGAP1 inhibiting amino acid signaling to mTORC1, overexpression of ArfGAP1 could also inhibit growth factor (insulin)-induced mTORC1 activation (Fig 2K). mTOR autophosphorylation on S2481, which serves as a biomarker for mTORC1 catalytic activity (Soliman *et al.*, 2010), did not appear to significantly change after the overexpression of ArfGAP1 (Figs 1E and 2K). Taken together, ArfGAP1 appears to be a negative regulator of mTORC1 activity.

### ArfGAP1 and mTORC1 interact in the absence of amino acids

Increased intracellular amino acid concentrations promote mTORC1 lysosomal localization and subsequent activation from an unknown location within the cell (Sancak *et al.*, 2008; Betz & Hall, 2013; Lawrence & Zoncu, 2019). Once mTORC1 is at the lysosome, it is activated allosterically by the small G protein Rheb, which is

downstream of growth factor signaling (Inoki *et al.*, 2003; Tee *et al.*, 2003; Zhang *et al.*, 2003; Yang *et al.*, 2017). Because ArfGAP1 and mTORC1 interact and co-localize in cells (Figs 1 and 3A), we investigated whether ArfGAP1 and mTORC1 bound better in the absence or presence of amino acids. Fluorescence lifetime imaging microscopy (FLIM) combined with Förster resonance energy transfer (FRET; FLIM/FRET) (Fig 3B and C) and Raster image cross-correlation spectroscopy (ccRICS) (Fig 3D) were used to examine the interaction between ArfGAP1 and Raptor in live-cells under different nutrient conditions. Specifically, endogenously GFP-tagged Raptor (Raptor-GFP) via CRISPR/Cas9 and overexpressed mCherry-tagged ArfGAP1 were observed for live-cell studies in wild-type or RagA/B KO HAP1 cells. Live-cell FLIM/FRET and ccRICS of GFP-tagged Raptor with mCherry-tagged ArfGAP1 indicated a small amount (< 10%) of ArfGAP1-Raptor interaction in cells when amino acids were present in the media (Fig 3B–D). In contrast, a significant increase in the binding between ArfGAP1 and mTORC1 (~15–35%) was observed in cells that were starved of amino acids (Fig 3B–D). Thus, ArfGAP1 and mTORC1 appear to co-localize more under amino acid-depleted conditions.

### ArfGAP1 regulates the lysosomal localization of mTORC1

Elevated amino acids promote mTORC1 lysosomal localization and subsequent activation (Sancak *et al.*, 2008). Currently, it is unclear where mTORC1 resides when it is not at the lysosome and amino acids are limiting (Betz & Hall, 2013; Lawrence & Zoncu, 2019). Because ArfGAP1 co-localizes with mTORC1 under amino acid starvation conditions (Fig 3), we hypothesized that ArfGAP1 may regulate mTORC1 lysosomal translocation. HA-tagged ArfGAP1 was expressed in mouse embryonic fibroblasts (MEFs) and mTOR lysosomal localization was assessed (Fig 4A). The co-localization of mTOR (green) and LAMP2 (red) were compared in cells expressing HA-tagged ArfGAP1 (positive) versus cells not expressing HA-tagged ArfGAP1 (negative). The expression of ArfGAP1 dramatically decreased mTOR and LAMP2 co-localization. Consistently, we saw a significant decrease in mTOR/LAMP2 co-localization in HEK293A cells when we expressed HA-tagged ArfGAP1, but not HA-tagged ArfGAP2 (Fig 4B). Consistently, knockdown of ArfGAP1 prevented

**Figure 3. Live-cell quantification of ArfGAP1-Raptor interaction under different nutrient conditions.**

- A *Left*—HA-tagged ArfGAP1 was transfected in RagA/B knockout (KO) human embryonic kidney 293A (HEK293A) cells. Immunofluorescence images of HA-tagged ArfGAP1 (green) and mTOR (red) were assessed for co-localization (scale bar, 5  $\mu$ m). *Right*—Line-scan analysis was performed. Yellow line (left) on image measures intensity along line. Distance across the yellow line is measured in microns.
- B Fluorescence lifetime imaging microscopy (FLIM) and Förster resonance energy transfer (FRET) analysis were performed in wild-type (WT, *left*) or RagA/B KO (*middle*) HAP1 cells expressing mCherry-tagged ArfGAP1 and endogenously GFP-tagged Raptor. Cells either had amino acids (+AA) or were starved of amino acids (–AA). At least 20 cells were analyzed in each group. Box plots show the percentage of pixels with  $\geq 30\%$  FRET efficiency of co-transfected cells. RFP1 was expressed and analyzed as a negative control. The whiskers of the boxplot represent the minimum and maximum values, while the box covers the data between 25<sup>th</sup> and 75<sup>th</sup> percentiles with a line in the middle plotted at the median. *Right*—Expression level of RagA/B was confirmed by Western blot analysis. Actin was used as a control.
- C Phasor analysis was performed for the FLIM/FRET experiments described in (B) in WT (*left*) or RagA/B KO (*right*) HAP1 cells expressing mCherry-tagged ArfGAP1 and endogenously GFP-tagged Raptor. Cells either had amino acids (+AA) or were starved of amino acids (–AA). For each condition, the first panel shows the fluorescence signal of the green channel. The second panel shows the phasor distribution of GFP (black circle), GFP-tagged Raptor (green circle), and GFP-tagged Raptor plus mCherry-tagged ArfGAP1 (red circle). The green line indicates where the GFP phasor would fall when containing autofluorescence. The third panel shows spatial distribution of pixels associated with FRET. Scale bars: 9  $\mu$ m for WT (*left*) and 5  $\mu$ m for RagA/B KO (*right*) cells, respectively.
- D Raster imaging correlation spectroscopy (RICS) analyses were performed for WT (*left*) or RagA/B KO (*right*) HAP1 cells expressing endogenously GFP-tagged Raptor (green curves) with either mCherry-tagged ArfGAP1 (blue curves) or RFP1 as a control (red curves). Auto-correlation (AC) or cross-correlation (CC) curves are shown for samples in conditions with amino acids (+AA, solid curve) or without amino acids (–AA, dashed curve).

Source data are available online for this figure.

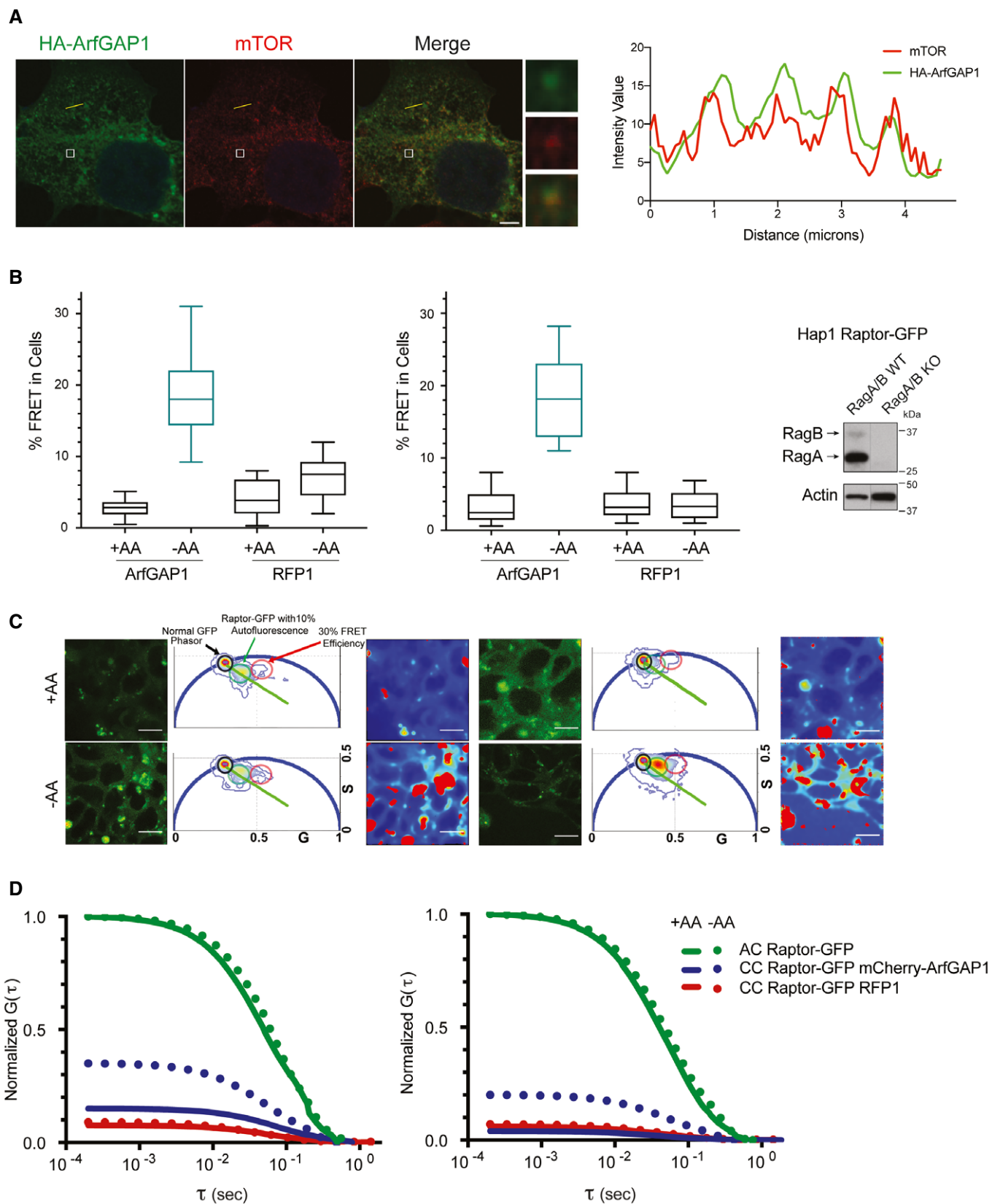


Figure 3.

the dissociation of mTORC1 away from the lysosomes under amino acid starvation conditions (Fig EV2). In addition, expression of ArfGAP1 also reduced mTOR localization to lysosomes under different nutrient conditions, such as amino acid starvation and re-stimulation (Fig 4B). Moreover, HA-tagged Raptor and endogenous ArfGAP1 co-immunoprecipitated to a stronger extent in amino acid-depleted conditions (Fig 4C). Based on these results and that depletion of ArfGAP1 renders cells resistance to amino acid withdrawal (Fig 2D and I), we reasoned that ArfGAP1 may sequester mTORC1 away from the lysosome, where mTORC1 could not become activated by Rheb. To support this, lysosome immunoprecipitations (Lyso-IPs) were performed where we immunopurified lysosomes from HEK293A cells expressing transmembrane protein 192 (TMEM192, lysosome localized protein) (Abu-Remaileh *et al.*, 2017). ArfGAP1 is not localized at the lysosome, like lysosomal-associated proteins RagA and the Ragulator component p18 (LAMTOR1), in amino acid-depleted cells or when cells have amino acids available (Fig 4D). Forcing mTORC1 to the lysosome near Rheb could perhaps bypass the inhibitory effect of ArfGAP1 on mTORC1. Indeed, artificially targeting of mTORC1 to the lysosomal surface by the addition of the C-terminal lysosomal targeting motif of Rheb (last 15 amino acids including the CAAX box) to Raptor (Sancak *et al.*, 2010; Jewell *et al.*, 2015) activated mTORC1 even when ArfGAP1 was overexpressed (Fig 4E). Thus, ArfGAP1 appears to play a role in the trafficking of mTORC1 to the lysosome and subsequent activation.

#### ArfGAP1 ALPS motifs are critical for mTORC1 regulation

Next, we investigated different ArfGAP1 regions in respect to interacting with and regulating mTORC1. ArfGAP1 has a conserved Arg (R50) in the N-terminal catalytic domain (Szafer *et al.*, 2000) important for GAP activity and two amphipathic lipid packing sensor (ALPS) motifs that sense vesicle membrane curvature (Mesmin

*et al.*, 2007) (Fig 5A). To investigate if the catalytic activity of ArfGAP1 is required for the ArfGAP1-mTORC1 interaction, we generated an inactive ArfGAP1 by mutating R50 to Lys (R50K) (Szafer *et al.*, 2000). Similar to the wild-type ArfGAP1, this catalytic inactive HA-tagged ArfGAP1 (HA-ArfGAP1<sup>R50K</sup>) could still bind to mTORC1 (Fig 5B). Next, to determine if ALPS motifs were important for ArfGAP1-mTORC1 binding, we mutated the ALPS motifs at Leu207 to Asp and Val279 to Asp (L207D/V279D). ALPS motifs of ArfGAP1 are important for the recruitment of ArfGAP1 to vesicles (Bigay *et al.*, 2003; Bigay *et al.*, 2005), and the L207D/V279D mutation has previously been shown to decrease the interaction of ArfGAP1 with liposomes *in vitro* (Mesmin *et al.*, 2007). Interestingly, the ArfGAP1 vesicle defective mutant (HA-ArfGAP1<sup>L207D/V279D</sup>) was unable to interact with mTORC1 in cells (Fig 5C). mTORC1 components (Flag-tagged mTOR, Flag-tagged Raptor, and Flag-tagged mLST8) were immunopurified from cells, and *in vitro* binding assays were performed with recombinant GST-tagged ArfGAP1 or GST-tagged ArfGAP1 L207D/V279D protein (Fig 5D). Interestingly, mTOR interacted the strongest with both ArfGAP1 and ArfGAP1 L207D/V279D, perhaps indicating a direct mTOR-ArfGAP1 interaction. These results suggest that the membrane curvature-sensing function, rather than the catalytic activity of ArfGAP1, is critical. Moreover, these results suggest that the ArfGAP1-mTORC1 complex may reside on the surface of a vesicle.

The C-terminus of ArfGAP1 has been reported to interact with two different types of coats involved in intracellular vesicle trafficking, the COPI complex and adaptor protein complex 2 (AP-2) (Yang *et al.*, 2002; Lee *et al.*, 2005; Bai *et al.*, 2011). Specifically, it has been reported that amino acids of rat ArfGAP1 301–400 (amino acids 301–394 of human ArfGAP1) interact with AP-2 and 401–415 (amino acids 395–406 of human ArfGAP1) interact with COPI (Bai *et al.*, 2011) (Fig 5A). COPI is involved in retrograde transport, where proteins are transported from the *cis* Golgi back to the rough ER (Faini *et al.*, 2013). In contrast, AP-2 is associated with clathrin

**Figure 4. ArfGAP1 inhibits mTORC1 by preventing its lysosomal translocation.**

- A Mouse embryonic fibroblast (MEF) cells were transfected with HA-tagged ArfGAP1. Immunofluorescence staining was assessed for HA-tagged ArfGAP1 (blue), mTOR (green), and LAMP2 (red, lysosomal marker). *Left*—A representative example of the immunofluorescence staining (scale bar, 10  $\mu$ m). The top left image shows the staining of HA-tagged ArfGAP1, with a white outline highlighting the region that is positive for HA-tagged ArfGAP1. This outline was overlaid with the mTOR channel (top right) and the LAMP2 channel (bottom left). The mTOR and LAMP2 channels were then merged and processed using the Squash segmentation algorithm (Rizk *et al.*, 2014; bottom right). The co-localization of mTOR and LAMP2 was analyzed for the region within the outline (HA-ArfGAP1 positive) and the region outside of the outline (HA-ArfGAP1-negative), respectively. *Right*—In each microscopy field, the image was processed as described above, and the co-localization between mTOR and LAMP2 was quantified and normalized by LAMP2-positive puncta using the Squash algorithm (Rizk *et al.*, 2014). The quantification was performed for the subgroups of cells that are positively or negatively stained for HA-tagged ArfGAP1, respectively, and compared using Student's *t*-test. Columns represent Mean  $\pm$  SEM ( $N = 3$ ).
- B Wild-type (WT) human embryonic kidney 293A (HEK293A) cells were transfected with HA-tagged ArfGAP1 or HA-tagged ArfGAP2 as a control. Cells were cultured under normal conditions (NC) or starved of amino acids (–AA) for 2 h, and then stimulated with amino acids (+AA) for 1 h. Immunofluorescence analysis was performed for HA-tagged ArfGAP1, HA-tagged ArfGAP2, mTOR, and LAMP2. In each microscopy field, the co-localization between mTOR and LAMP2 (normalized by the LAMP2-positive puncta) was quantified for HA-tagged ArfGAP1-positive or -negative or HA-tagged ArfGAP2-positive or -negative cell populations, respectively. Bar plot shows Mean  $\pm$  SEM ( $N = 8–10$ ). *P* values were determined using Student's *t*-test, and ns denotes for not significant.
- C HEK293A cells were transfected with HA-tagged Raptor. Cells were cultured under normal condition (NC) or starved of amino acids (–AA) for 2 h. Endogenous ArfGAP1 was immunoprecipitated. IP or whole cell lysate (WCL) samples were probed for HA, ArfGAP1, the phosphorylated S6K1 at threonine 389 (pS6K1), S6K1, and Actin served as a loading control.
- D MIA Paca-2 cells stably expressing Flag-tagged or HA-tagged TMEM192 were cultured under normal condition (NC) or starved of amino acids (–AA) and then stimulated with 2 mM glutamine and asparagine (+Gln/Asn) for 2 h. HA-tagged TMEM192 was immunoprecipitated with HA beads and IP and WCL were probed for ArfGAP1, HA, RagA, or p18 (LAMTOR1). Flag, pS6K1 at threonine 389 (mTORC1 activity), S6K1, and Vinculin were probed for as controls.
- E RagA/B knockout (KO) HEK293A cells were co-transfected with HA-tagged ArfGAP1 or EGFP (control) with HA-tagged Raptor or HA-tagged Raptor fused with C-terminus region of Rheb (HA-Raptor-C-Rheb), and Myc-tagged S6K1. Cells were starved of amino acids (–AA) for 2 h, and then, 4 mM of glutamine (+Gln) or asparagine (+Asn) was added for 2 h. Cell lysate was immunoprecipitated with anti-Myc beads. IP or WCL samples were probed for HA, Myc, and phosphorylated S6K1 at threonine 389 (pS6K1; mTORC1 activity). Actin served as a loading control.

Source data are available online for this figure.



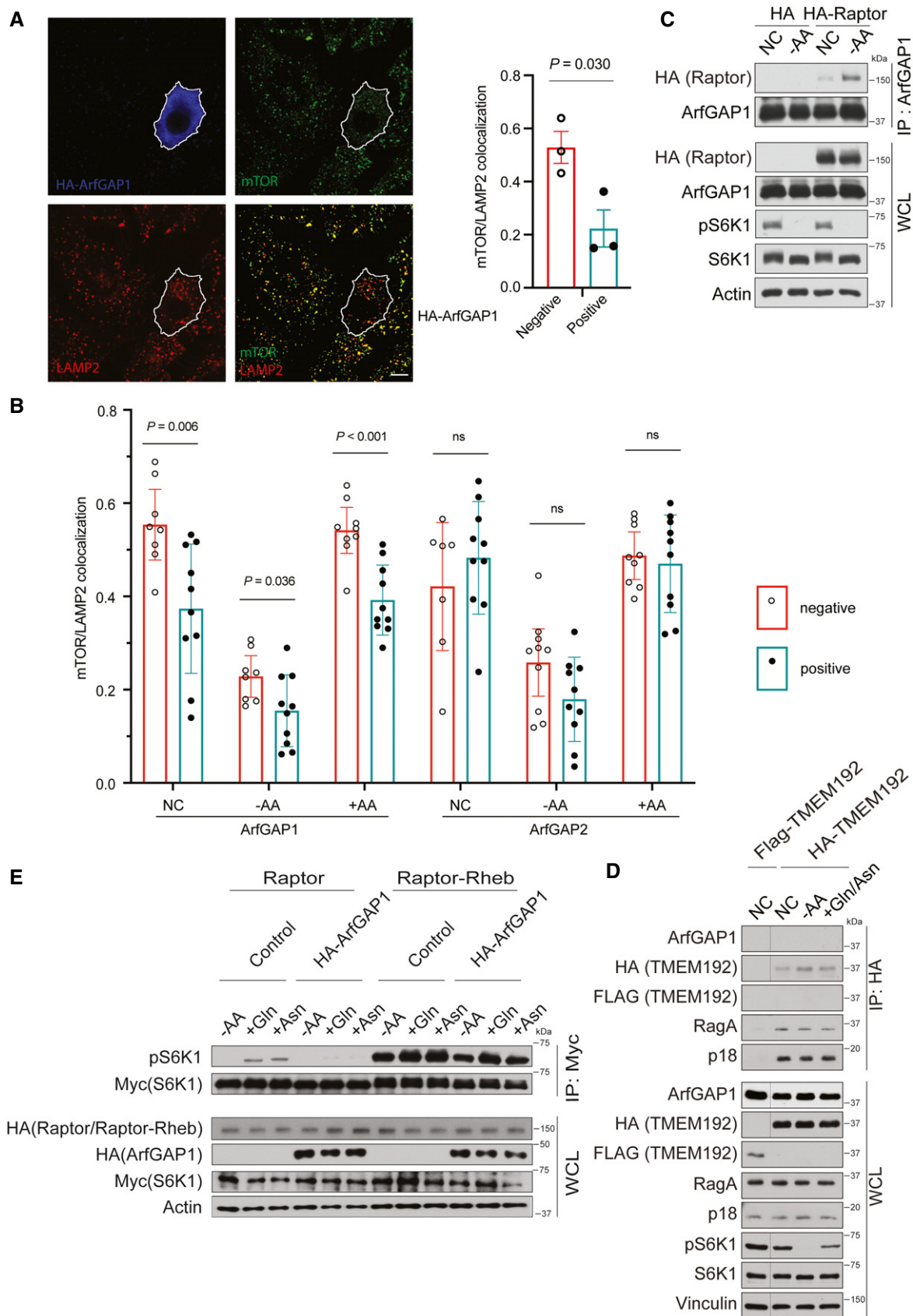


Figure 4.

and is thought to be involved in endocytosis, forming vesicles at the plasma membrane that are transported into early endosomes (Faini *et al*, 2013). To investigate if binding to any of these coat proteins may play a role in the ArfGAP1-mTORC1 interaction, we first attempted to disrupt the AP-2 interaction function of ArfGAP1. Previous work revealed that when rat ArfGAP1 was mutated at Phe332Ala/Trp366Ala/Trp385Ala (FWW), ArfGAP1 was deficient in binding to AP-2 but not COPI (Bai *et al*, 2011). Rat ArfGAP1 only shares Phe332 and Trp367 with human ArfGAP1 (Fig EV3A), so we mutated Phe332 to Ala and Trp367 to Ala (FW) in human ArfGAP1 and assessed the ability of HA-tagged ArfGAP1<sup>FW</sup> to bind to coat proteins. As expected, wild-type ArfGAP1 conferred interaction with both  $\beta$ -COP (a subunit of the COPI complex) and AP-2, whereas the ArfGAP1 FW mutant did not bind to AP-2 (Fig EV3B). However, ArfGAP1 FW also failed to interact with  $\beta$ -COP, with the reason currently unclear. Because the C-terminus of ArfGAP1 (amino acids 395–406 of human ArfGAP1) interacts with COPI (Fig 5A) (Bai *et al*, 2011), we generated an HA-tagged ArfGAP1 missing the COPI-interacting domain (HA-tagged ArfGAP1<sup>1–394</sup>). As expected, co-immunoprecipitation experiments revealed that HA-tagged ArfGAP1<sup>1–394</sup> could still interact with AP-2, but not  $\beta$ -COP (Fig 5E). To determine whether or not the COPI interaction was involved in ArfGAP1-mTORC1 binding, HA-tagged ArfGAP1<sup>1–394</sup> was co-immunoprecipitated and mTORC1 binding was assessed. ArfGAP1<sup>1–394</sup> could still confer interaction with mTORC1 (Fig 5F). Thus, COPI binding is not required for the ArfGAP1-mTORC1 interaction.

We tested if the catalytic activity, ALPS motifs, or COPI binding domain were required for ArfGAP1 to regulate mTORC1 signaling. Consistent with the requirement of the ALPS motifs for the ArfGAP1-mTORC1 interaction, we found that the ALPS motifs are also crucial for ArfGAP1 to repress mTORC1 signaling, as the ArfGAP1 ALPS mutant (HA-ArfGAP1<sup>L207D/V279D</sup>) was unable to inhibit mTORC1 activation (Figs 5G and EV3C). As for the catalytic activity of ArfGAP1, expression of HA-tagged ArfGAP1 mutant (ArfGAP1<sup>R50K</sup>) and the COPI defective binding mutant of ArfGAP1 (ArfGAP1<sup>1–394</sup>) could still inhibit mTORC1, to some extent (Fig EV3C). Taken together, the membrane curvature-sensing function is crucial for ArfGAP1 to regulate mTORC1 signaling.

The membrane curvature-sensing ALPS motifs of ArfGAP1 play a role in mTORC1 interaction and repression (Fig 5), suggesting that ArfGAP1 might be on some vesicles when it inhibits mTORC1. Because ArfGAP1 regulates AP-2 and clathrin-dependent endocytosis (Bai *et al*, 2011), we investigated if AP-2 or clathrin played a role in ArfGAP1-mediated mTORC1 repression. We reasoned that if AP-2 or clathrin were required for ArfGAP1 to function, deletion of AP-2 or clathrin would rescue the inhibition of mTORC1 by ArfGAP1 overexpression. However, effective knockdown of clathrin heavy chain (CHC; Fig EV4A and B) or AP-2  $\mu$  subunit (AP2M1; Fig EV4C) did not affect mTORC1 inhibition by ArfGAP1. Furthermore, knockdown of other AP-2 subunits did not alter mTORC1 signaling (Fig EV4D). Clathrin consists of 3 heavy chains and 3 light chains, and forms the “cage” of vesicles through its triskelion-shape structure (Faini *et al*, 2013). AP-2 and other AP complexes are heterotetramers consisting of two large subunits or adaptins ( $\alpha$  and  $\beta$  for AP-2), one medium adaptin ( $\mu$ ), and one small adaptin ( $\sigma$ ) (Sanger *et al*, 2019). Because there are multiple AP complexes and they share similarity in sequences and structure (Sanger *et al*, 2019), we tested if ArfGAP1 can also interact with other AP complexes (Fig EV4E). HA-tagged ArfGAP1, but not HA-tagged ArfGAP2, bound to five AP complexes (AP-1 to AP-5), indicating potential involvement of AP complexes other than AP-2. Taken together, AP-2 complexes do not appear to play a role in ArfGAP1's ability to inhibit mTORC1.

### ArfGAP1 regulates pancreatic cancer cell growth and predicts clinical outcomes

We next asked if ArfGAP1 plays a role in human diseases where mTORC1 is hyperactivated. Given the critical role of mTORC1 signaling in cancer development and progression (Blenis, 2017; Mossmann *et al*, 2018; Liu & Sabatini, 2020), we hypothesized that alterations of ArfGAP1 might be involved in cancer. By analyzing The Cancer Genome Atlas (TCGA) dataset, we found that ArfGAP1 is a predictive factor for pancreatic cancer. Patients with high levels of ArfGAP1 have a significant favorable clinical outcome (median overall survival (OS) = 22.7 months) compared with patients with

#### Figure 5. ALPS motifs are crucial for ArfGAP1 to interact with and inhibit mTORC1.

- Schematic of domain distribution of wild-type human ArfGAP1 (amino acids 1–406) and the COPI defective mutant of ArfGAP1 (amino acids 1–394). Critical residues of various domains are highlighted.
- RagA/B knockout (KO) human embryonic kidney 293A (HEK293A) cells were transfected with HA-tagged wild-type ArfGAP1, the HA-tagged ArfGAP1 R50K mutant, or empty vector (EV, control) for 72 h. Cell lysates were immunoprecipitated with anti-HA beads. Immunoprecipitates (IP) or whole cell lysate (WCL) samples were probed for HA and mTORC1 components (mTOR, Raptor, and mLST8). Vinculin was probed for as a control.
- RagA/B KO HEK293A cells were transfected with HA-tagged wild-type ArfGAP1, HA-tagged ArfGAP1 L207D/V279D, or RFP1 (control) for 24 h. Cell lysates were immunoprecipitated with anti-HA beads and analyzed as in (B).
- Top*—Input of GST, GST-tagged ArfGAP1, and GST-tagged ArfGAP1 L207D/V279D that was used in the *in vitro* binding assays. *Bottom*—Flag-tagged mTOR, Flag-tagged Raptor, and Flag-tagged mLST8 were overexpressed in HEK293A cells. Cell lysates were immunoprecipitated with anti-Flag beads and incubated with either GST (control), GST-tagged ArfGAP1, or GST-ArfGAP1 L207D/V279D. IP or WCL samples were probed for Flag or GST.
- RagA/B KO HEK293A cells were transfected with HA-tagged wild-type ArfGAP1, 1–394 truncation of ArfGAP1, or RFP1 as a control for 24 h. Cell lysates were immunoprecipitated with anti-HA beads. IP or WCL samples were probed for HA, AP-2, or  $\beta$ -COP. Actin served as a loading control.
- RagA/B KO HEK293A cells were transfected with HA-tagged ArfGAP1, HA-tagged ArfGAP1 1–394, or RFP1 (control) for 24 h. Cell lysates were immunoprecipitated with anti-HA beads. Cell lysates were analyzed as in (B).
- RagA/B KO HEK293A cells were co-transfected with HA-tagged ArfGAP1, HA-tagged ArfGAP1 L207D/V279D, or RFP1 (control) together with Myc-S6K1. Cells were starved of amino acids (–AA) for 2 h, and then, 4 mM of Gln or Asn was added for 2 h. Cell lysate was immunoprecipitated with anti-Myc beads. IP or WCL samples were probed for HA, Myc, and phosphorylated S6K1 at threonine 389 (pS6K1). Actin served as a loading control.

Source data are available online for this figure.

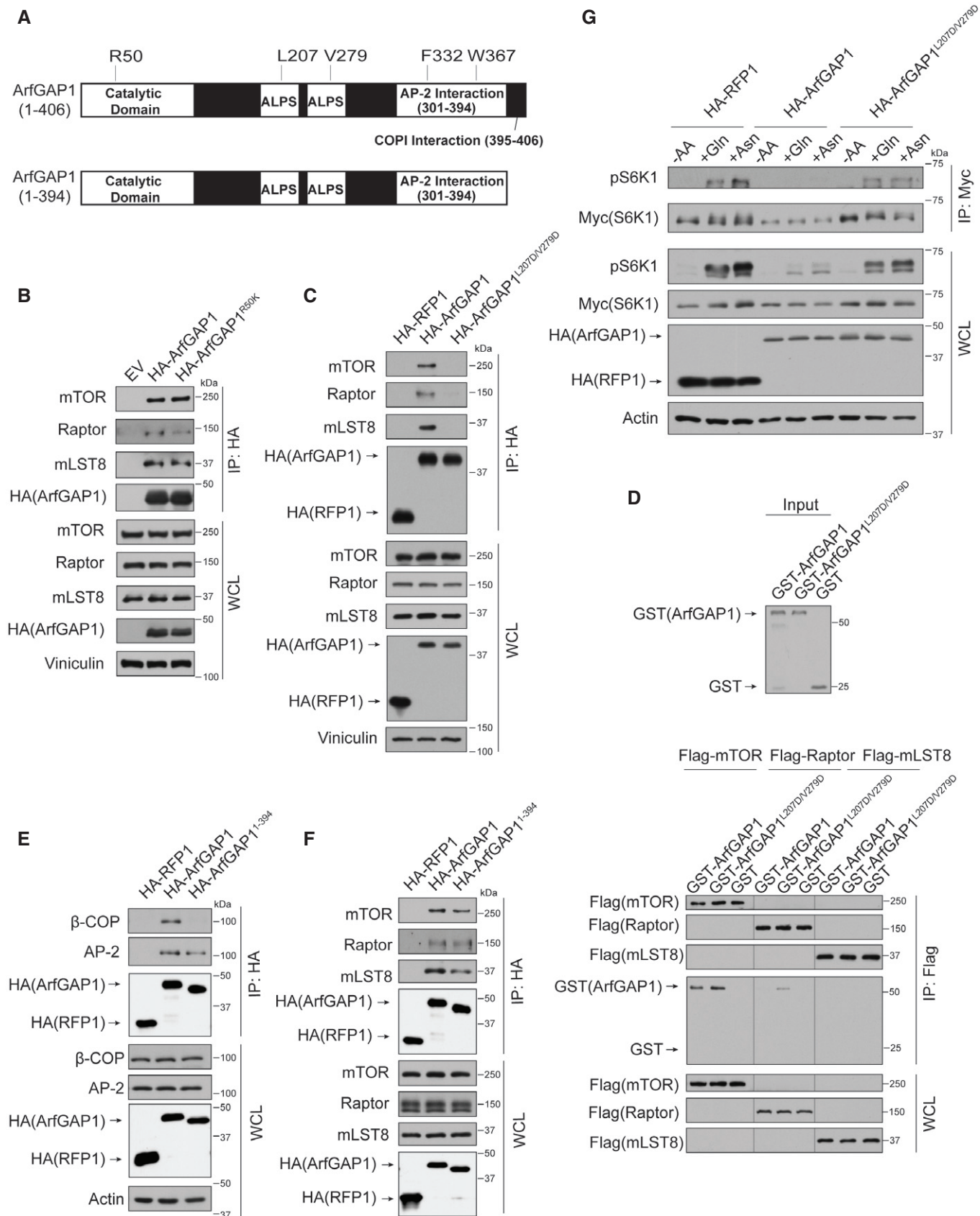
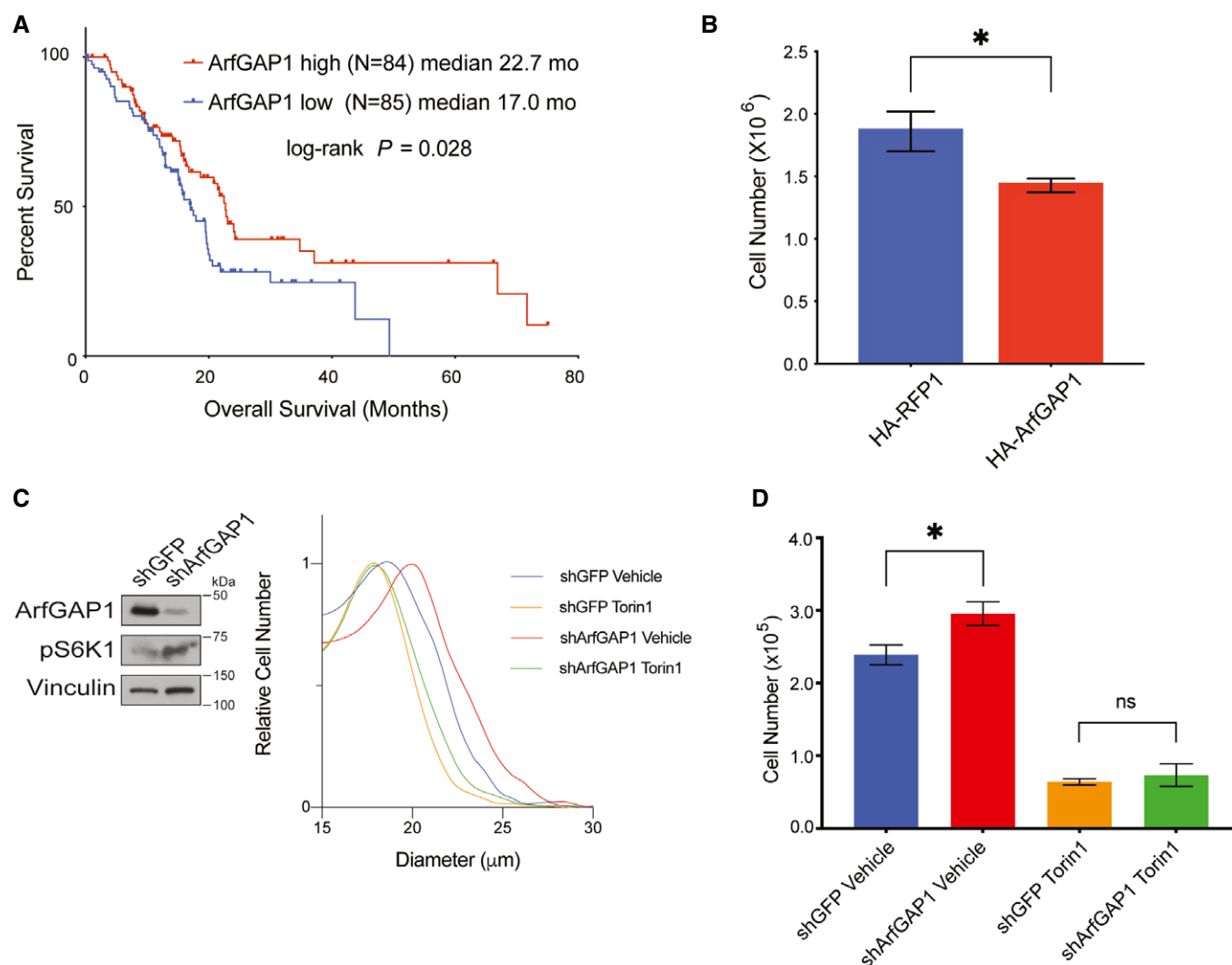


Figure 5.

lower levels of ArfGAP1 (median OS = 17.0 months) (Fig 6A). Moreover, after adjusting clinical features that are known to be associated with pancreatic cancer survival, such as age at diagnosis, gender, primary tumor site, grade, resection extent, clinical stage,

lymph nodes, ArfGAP1 is still an independent prognosis predictor for favorable overall survival (Table 1).

To further determine the role of ArfGAP1 in mTORC1-mediated physiology (Blenis, 2017; Mossmann *et al*, 2018; Liu & Sabatini,



**Figure 6. ArfGAP1 is associated with more favorable clinical outcome of pancreatic cancer patients and suppresses pancreatic cancer growth.**

**A** TCGA cohort of pancreatic cancer patients were divided into two groups according to the median level of ARFGAP1 mRNA expression. Overall survival was compared between these two groups, as shown in Kaplan–Meier curves. Median survivals (in months) and log-rank  $P$  values are indicated.

**B** MIA Paca-2 cells were transfected with HA-tagged ArfGAP1 or RFP1 (control) for 4 days, and then, cell numbers were counted. Six replicated wells were counted each group. Columns represent Mean  $\pm$  SEM. Student's  $t$ -test  $*P = 0.028$ .

**C** *Left*—Expression levels of ArfGAP1 and phosphorylation of S6K1 (pS6K1) at threonine 389 (mTORC1 activity) were analyzed by immunoblotting in MIA Paca-2 cells stably expressing short hairpin RNAs (shRNAs) against ArfGAP1 or GFP (control). Vinculin was a loading control. *Right*—MIA Paca-2 cells stably expressing short hairpin RNAs (shRNAs) against ArfGAP1 or GFP as a control were treated with mTOR inhibitor Torin 1 (250 nM) or vehicle control for 24 h, and then, cell diameters were determined using a particle size counter. The curves show the overall distribution of cell size in each group. Mean of average size  $\pm$  SD ( $N = 4$ ): shGFP Vehicle  $19.55 \pm 0.10$ , shGFP Torin 1  $18.76 \pm 0.12$ , shArfGAP1 Vehicle  $20.63 \pm 0.16$ , shArfGAP1 Torin 1  $19.05 \pm 0.09$ . Student's  $t$ -test  $P$  values: shGFP Vehicle versus shGFP Torin 1 ( $P = 4.891\text{E-}05$ ), shGFP Vehicle versus shArfGAP1 Vehicle ( $P = 2.546\text{E-}05$ ), shArfGAP1 Vehicle versus shArfGAP1 Torin 1 ( $P = 2.38\text{E-}06$ ), and shGFP1 Torin 1 versus shArfGAP1 Torin 1 ( $P = 0.007$ ).

**D** MIA Paca-2 cells stably expressing shRNAs against ArfGAP1 or GFP (control) were plated and treated with mTOR inhibitor Torin 1 (250 nM) or vehicle control for 48 h prior to cell counting. Columns represent Mean  $\pm$  SEM ( $N = 6$ ). Student's  $t$ -test shGFP Vehicle versus shGFP Torin 1 ( $P = 2.83\text{E-}07$ ), shGFP Vehicle versus shArfGAP1 Vehicle ( $*P = 0.025$ ), shGFP Torin 1 versus shArfGAP1 Torin 1 ( $P = 0.139$ ), and shArfGAP1 Vehicle versus shArfGAP1 Torin 1 ( $P = 1.22\text{E-}07$ ). “ns” stands for “not significant”.

Source data are available online for this figure.

**Table 1. Univariate and multivariate Cox proportional hazards regression models for overall patient survival of TCGA PDAC cohort.**

Characteristics	Univariate cox regression		Multivariate cox regression	
	HR (95% CI)	P-value	HR (95% CI)	P-value
Age (Years)	1.02 (1.00–1.04)	<b>0.048</b>	1.03 (1.01–1.05)	<b>0.006</b>
Gender (Male versus Female)	0.77 (0.51–1.16)	0.208		
Primary Tumor Site (Head versus Others)	1.76 (0.97–3.18)	0.061		
Grade (G3/4 versus G1/2)	1.31 (0.85–2.01)	0.228		
Resection (R1 versus R0)	1.71 (1.09–2.67)	<b>0.019</b>	1.58 (0.99–2.53)	0.056
T Stage (T3/4 versus T1/2)	1.20 (0.64–2.26)	0.572		
N Stage (N1 versus N0)	1.84 (1.09–3.08)	<b>0.021</b>	1.34 (0.72–2.50)	0.356
Lymph Nodes (Positive versus Negative)	1.08 (1.02–1.14)	<b>0.008</b>	1.06 (0.98–1.14)	0.134
ArfGAP1 (High versus Low)	0.63 (0.41–0.95)	<b>0.029</b>	0.60 (0.39–0.95)	<b>0.027</b>

CI, confidence interval; HR, hazard ratio.  
P-values less than 0.05 are considered statistically significant and shown in bold.

2020) and pancreatic cancer, we expressed ArfGAP1 in HEK293A cells, the human pancreatic cancer cell line MIA Paca-2, and the mouse pancreatic cancer cell line mouse PaCa. Cell proliferation and size was assessed for mTORC1 biology. Consistent with the fact that mTORC1 promotes cell proliferation and cell size as previously reported (Fingar *et al*, 2002; Fingar *et al*, 2004), we found that expression of HA-tagged ArfGAP1 significantly reduced cell proliferation and size (Figs 6B and EV5A–C). In contrast, knockdown of ArfGAP1 dramatically enhanced cell proliferation and cell size (Figs 6C and D, and EV5D). Treatment of cells with the mTOR inhibitor Torin1 reversed these phenotypes (Fig 6C and D). Thus, ArfGAP1 is crucial in the regulation of pancreatic cancer cell growth and is an independent prognostic factor for clinical outcome of pancreatic cancer.

## Discussion

mTORC1, known as “the master regulator”, promotes protein synthesis, lipid metabolism, and cell growth (Ben-Sahra & Manning, 2017; Gonzalez & Hall, 2017; Meng *et al*, 2018). The cellular localization of mTORC1 is critical for its activation, and intracellular membrane trafficking plays a role in mTORC1 trafficking to and from the lysosome (Sancak *et al*, 2008; Flinn *et al*, 2010; Li *et al*, 2010; Betz & Hall, 2013; Jewell *et al*, 2015). Under amino acid-depleted conditions, mTORC1 is dispersed in a diffused pattern throughout the cell at an undefined location (Sancak *et al*, 2008; Sancak *et al*, 2010; Bar-Peled *et al*, 2012). In contrast, in the presence of amino acids mTORC1 is shuttled to the lysosome where it interacts with and is activated by Rheb (Sancak *et al*, 2008; Sancak *et al*, 2010; Bar-Peled *et al*, 2012). How mTORC1 is trafficked to the lysosome in response to amino acids, and where it is localized in the cell in the absence of amino acids is currently unclear (Betz & Hall, 2013).

In this study, we identified ArfGAP1 as a crucial component involved in amino acid signaling to mTORC1. Our data reveal that ArfGAP1 interacts with mTORC1 in the absence of amino acids (Fig 7). Elevated levels of ArfGAP1 potently inhibit amino acid-induced mTORC1 activation, likely by sequestering mTORC1 away

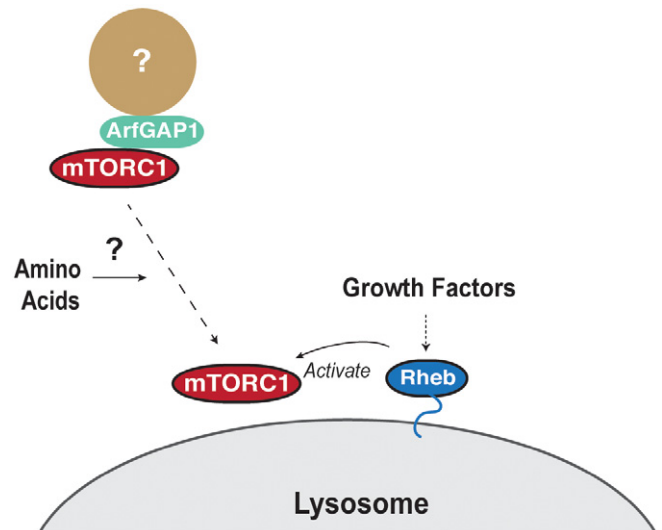


**Figure 7. Model of ArfGAP1 suppressing mTORC1 lysosomal translocation and activation.**

Amino acids promote the translocation of mTORC1 to lysosomes. On lysosomal surface, mTORC1 can be activated by the small GTPase Rheb downstream of the growth factor signaling. In this study, we discovered that ArfGAP1 interacts mTORC1, likely on some unknown membrane vesicles through its ALPS motifs (not shown here), and inhibits the lysosomal translocation and activation of mTORC1.

from the lysosome. Consistently, depletion of ArfGAP1 enhances mTORC1 lysosomal localization, activation, and signaling. The ALPS motifs of ArfGAP1, which are required for membrane curvature-sensing, are critical in order for ArfGAP1 to interact with and regulate mTORC1 activity. Importantly, ArfGAP1 appears to play a critical role in mTORC1-mediated biology such as pancreatic cancer.

Rat ArfGAP1 was cloned as the first GAP for Arf proteins 25 years ago (Cukierman *et al*, 1995; Makler *et al*, 1995), and the function of ArfGAP1 has been intensively studied. Most research on ArfGAP1 is focused on COPI-mediated retrograde membrane trafficking from the Golgi apparatus to ER, where ArfGAP1 serves as a



GAP for Arf1. Importantly, ArfGAP1 appears to have many more biological implications. For example, other than acting as a GAP for Arf1, ArfGAP1 also serves as an effector protein, recruiting cargo proteins as component of the coat complexes to form vesicles (Yang *et al*, 2002; Lee *et al*, 2005). Second, besides the well-elucidated role in Arf1 and COPI-mediated Golgi-ER transport, ArfGAP1 is involved in other processes of membrane trafficking. ArfGAP1 was shown to promote AP-2-dependent endocytosis, acting as an Arf6 regulator in AP-2 transport (Bai *et al*, 2011). In addition, ArfGAP1 has also been reported to be genetically associated with AP-3 complex in *Drosophila* (Rodriguez-Fernandez & Dell'Angelica, 2015). Third, the GAP activity of ArfGAP1 is not restricted to Arf family proteins. ArfGAP1 can regulate the GTPase activity of other small GTPases such as leucine-rich repeat kinase 2 (LRRK2), a critical multi-function protein associated with Parkinson's disease (Stafa *et al*, 2012; Xiong *et al*, 2012).

This study shows for the first time that ArfGAP1 regulates mTORC1 lysosomal localization and subsequent activation. Our data show that the GAP activity of ArfGAP1 does not appear to be required for mTORC1 regulation, whereas the ALPS motifs of ArfGAP1 are critical for both the interaction and activity of mTORC1. Moreover, altering the guanine nucleotide loading of Arf1 does not rescue ArfGAP1-induced mTORC1 inhibition. ArfGAP1 interacts with mTORC1 away from the lysosome in the absence of amino acids, preventing lysosomal localization and activation. Unlike other ArfGAPs, ArfGAP1 specifically binds to membranes on small vesicles through its two unique lipid packing sensor (ALPS) motifs (Bigay *et al*, 2003; Bigay *et al*, 2005; Mesmin *et al*, 2007). Mutations in these two ALPS motifs rendered ArfGAP1 unable to interact with and control mTORC1 activity. Thus, membrane curvature recognition and binding appear to be crucial for ArfGAP1 to recruit and repress mTORC1. Out of the ~30 mammalian ArfGAPs, ArfGAP1 is the only one that contains ALPS motifs. ArfGAP2 and ArfGAP3 are closest to ArfGAP1 in sequence similarity. However, ArfGAP2 and ArfGAP3 do not have ALPS motifs and have to be recruited to membranes by other proteins (Jackson & Bouvet, 2014).

Interestingly, a truncated ArfGAP1 (missing the C-terminus region) that cannot bind to COPI (Rawet *et al*, 2010; Bai *et al*, 2011) is still capable of repressing mTORC1 suggesting that the role of ArfGAP1 in COPI transport is not required for mTORC1 regulation. Our data also ruled out the involvement of AP-2 complex in ArfGAP1's regulation on mTORC1. However, ArfGAP1 could potentially bind other type of AP complexes when it interacts with and inhibits mTORC1. Thus, more mechanistic details of ArfGAP1's role in inhibiting mTORC1 warrant further investigation in the future. For example, what specific type of vesicles ArfGAP1 recruits mTORC1 to and what other proteins are involved. The biochemical function of ArfGAP1 has been widely studied using *in vitro* assays. However, our understanding of the involvement of ArfGAP1 in physiological settings, particularly in respect to nutrient sensing, mTORC1 regulation, and human diseases, is rather limited. Here we found ArfGAP1 as a critical regulator of mTORC1 signaling, cell growth, and pancreatic cancer. Importantly, expression levels of ArfGAP1 are an independent prognostic factor for clinical outcome of pancreatic cancer patients. Thus, our study may provide insights into novel strategies to perturb mTORC1 activity in pancreatic cancer treatment.

## Materials and Methods

### Antibodies and chemicals

The following antibodies were purchased from Cell Signaling Technology and used at the indicated dilution for Western blot analysis: phospho-S6K1 (Thr389; #9234, 1:1,000), S6K1 (#9202, 1:1,000), phospho-mTOR (Ser 2481; #2974, 1:1,000), mTOR (#2972, 1:1,000), Raptor (#2280, 1:1,000), mLST8 (#3274, 1:1,000), DEPTOR (#11816, 1:1,000), PRAS40 (#2691, 1:1,000), RagA (#4357, 1:1,000), ARFGAP1 (#14608, 1:1,000), phospho-4EBP1 (Ser65; #9451, 1:1,000), Vinculin (#4650, 1:1,000) and Actin (#3700, 1:100,000). Flag (#F3165, 1:10,000) and  $\beta$ -COP (#G2279, 1:1,000) were obtained from Sigma. AP-1 (#sc-398867, 1:1,000), AP-2 Adaptin 1/2 (#sc-17771, 1:2,000), AP-3 (#sc-136277, 1:1,000), AP-4 (#sc-135835, 1:1,000), CHC (#sc-12734, 1:1,000), HA (#sc-7392, 1:500) and Myc (#sc-40, 1:1,000) were obtained from Santa Cruz. AP-5 (#HPA035693, 1:1,000) antibody was obtained from Atlas Antibodies. GFP antibody (#632381, 1:2,000) was obtained from Clontech. Horseradish peroxidase (HRP) linked secondary antibodies (#NXA931V anti-mouse or #NA934V anti-rabbit, 1:4,000) were from GE Healthcare.

Antibodies used for the immunofluorescence microscopy experiments: mTOR (#2983, 1:200) and phospho-S6 (Ser235/236) Alexa Fluor 555 conjugate (#3985, 1:200) were purchased from Cell signaling. HA (#sc-805-G, 1:200) and HA Alexa Fluor 488 conjugate (#s-805 AF488, 1:100) were obtained from Santa Cruz. Alexa Fluor 488 and 647 secondary antibodies (1:200) were obtained from Invitrogen.

Brefeldin A (#B6542), insulin (#I1507) and Torin 1 (#475991) were from Sigma.

### Cell lines and tissue culture

Human embryonic kidney 293A (HEK293A) cells, mouse embryonic fibroblasts (MEFs), MIA Paca-2 human pancreatic cancer cells, and mouse pancreatic cancer (mouse PaCa) cells were cultured in high-glucose DMEM (#D5796 from Sigma). HAP1 human near-haploid cells were cultured in IMDM (#I3390 from Sigma). All cells were cultured in media supplemented with 10% FBS (#F2442 from Sigma) and penicillin/streptomycin (#P0781 from Sigma, 100 units penicillin and 100  $\mu$ g streptomycin/ml), and maintained at 37°C with 5% CO<sub>2</sub>. RagA/B KO MEFs and HEK293A cells were generated previously (Jewell *et al*, 2015). MIA Paca-2 cell line was a generous gift from Dr. Kim Orth at UT Southwestern Medical Center. The mouse PaCa cell line is a primary line derived from a *LSL-Kras*<sup>G12D/+</sup>; *Trp53*<sup>fl/fl</sup>; *Pdx1*<sup>Cre</sup> (*KPfc*) pancreatic cancer mouse model and was a generous gift from Dr. Rolf Brekken at UT Southwestern Medical Center. Wild-type HAP1 and HAP1 endogenously expressing Raptor-GFP cell lines were generous gifts from Dr. Nicholas Ktistakis at Babraham Institute (Manifava *et al*, 2016).

For the generation of RagA/B KO HEK293A cells stably expressing Flag-tagged Raptor, a retroviral vector (pQCXIP backbone) encoding Flag-Raptor was transfected in HEK293A cells, together with a packaging plasmid pCL10A, and the produced recombinant retroviruses were collected from the medium 48 h after transfection. RagA/B KO HEK293A cells were then infected with the recombinant retroviruses with 5  $\mu$ g/ml polybrene (TR-1003-G from Millipore), followed by selection of infected cells using puromycin (5  $\mu$ g/ml; #ant-pr-1 from InvivoGen).



Mouse Paca cells stably overexpressing HA-ArfGAP1 were generated similarly by infection of lentiviruses produced by co-transfection of lenti-blast-HA-ArfGAP1 and packaging plasmids pMD2.G and pSPAX2. Cells were selected using blasticidin (10 µg/ml; #A1113903 from Thermo Fisher Scientific).

### Plasmids and cDNA transfection

The cDNA for human ARFGAP1 (NM\_018209.2) was obtained from the McDermott Center for Human Genetics in UT Southwestern Medical Center, amplified using Q5 high-fidelity DNA polymerase (#M0492L from New England Biolabs) and subcloned into *Sall* and *EcoRI* sites of pRK7. An HA tag was fused to the N terminus of the protein product. HA-RFP1, HA-ArfGAP2, and truncation of HA-ArfGAP1 were generated similarly. Mutations were introduced by site-directed mutagenesis. HA-Raptor and HA-Raptor-C-Rheb (Raptor fused to C-terminal of Rheb), HA-tagged wild-type and mutated Arf1 (GTP-bound and GFP-bound) were previously generated (Jewell et al, 2015). A Flag tag was fused to Raptor and subcloned to pRK7 or pQCXIP backbones. All constructs used were verified by DNA sequencing. HA-ArfGAP1 was subcloned into lentiCas9-Blast (Addgene #52962 (Sanjana et al, 2014); a kind gift from Feng Zhang) for lentivirus production and stable cell line generation.

Cells were transfected with plasmid DNA using PolyJet™ DNA *In Vitro* Transfection Reagent (#SL100688 from SignaGen Laboratories) according to manufacturer's instructions. HEK293A cells were seeded into culture dishes approximately 24 h prior to transfection. For co-immunoprecipitation experiments, cells were plated in 10cm dishes and transfected with 6 µg of HA-ArfGAP1 or other plasmids as indicated. Fresh medium was replaced 6 h after the transfection, and samples were harvested 24 h later. For co-transfection experiment to test mTORC1 activity, cells were plated in 6-well plates and co-transfected with 25 ng of Myc-S6K1 and 1–2 µg of HA-ArfGAP1 or other plasmids as indicated. Fresh medium was replaced 6 h after the transfection. 72–96 h post-transfection, cells were starved of amino acids and stimulated with indicated amino acids, and samples were collected for immunoprecipitation.

### Amino acid starvation and stimulation of cells

Amino acid-free medium was made following the Sigma (#D5796) high-glucose DMEM recipe with the exception that all amino acids were omitted. All experiments with amino acid starvation and stimulation contained 10% dialyzed FBS (#F0392 from Sigma) instead of regular FBS (#F2442 from Sigma). Amino acid starvation was performed by replacing regular medium with amino acid-free medium for indicated time. For amino acid stimulation experiments, cells were first starved of amino acids for approximately 1–2 h. Then amino acids were added with indicated concentration and time points. All amino acids were obtained from Sigma.

### Cell lysis and immunoprecipitation

Cells were rinsed with ice-cold PBS and lysed in ice-cold CHAPS lysis buffer [40 mM HEPES pH 7.5, 10 mM pyrophosphate, 10 mM glycerophosphate, 2.5 mM MgCl<sub>2</sub>, 0.3% CHAPS, and EDTA-free protease inhibitors (#11873580001 from Roche; one tablet per 25 ml)] for the co-immunoprecipitation experiment, or Triton lysis

buffer (1% Triton X-100 instead of 0.3% CHAPS for the above recipe) for the Myc-S6K1 co-transfection experiment. The soluble fractions from cell lysates were isolated by centrifugation at 21,000 g for 10 min in a microfuge at 4°C. 50 µl of cell lysate was taken as an input control. For immunoprecipitations in HEK293A cells, around 30 µl of anti-HA (#PI88836 from Thermo Fisher Scientific), Flag (#A2220 from Sigma), or Myc (#20168 from Thermo Fisher Scientific) beads were added to each sample and incubated with rotation for 2 h to overnight at 4°C. For HAP1 cells expressing endogenous Raptor-GFP, GFP antibody was added at 1:85 dilution at 4°C overnight, followed by 4-h incubation of 40 µl of protein A/G beads (#PI88802 from Thermo Fisher Scientific). Immunoprecipitates were washed three times with lysis buffer (containing 150 mM NaCl or 500 mM NaCl for Myc-S6K1 experiment). Immunoprecipitated proteins were denatured by adding around 50 µl of sample buffer and boiling for 5–10 min, resolved by 10–15% SDS-PAGE, and analyzed via Western blot analysis.

### Lysosome immunoprecipitation

Mia Paca-2 cells stably expressing Flag-tagged or HA-tagged TMEM192 were plated in 2 of 15cm plates for the following conditions: normal condition (NC), amino acid starvation (–AA), or amino acid starvation plus glutamine/asparagine (+Gln/Asn). Complete media was used to normalize the cells for 1 h before starvation. Cells were then starved for 2 h or starved then stimulated with 2 mM Gln/Asn each. Cells were then collected and immunoprecipitated using HA beads (Thermo Fisher Scientific, #88836) overnight in CHAPS lysis buffer. More details for the immunoprecipitation of lysosomes (Lyso-IP) can be found here (Abu-Remaileh et al, 2017).

### Protein purification

The human ArfGAP1 (or ArfGAP1 L207D/V279D) coding sequence was cloned into a pGEX4T-1 vector containing an N-terminal GST-tag. Rosetta (BL21 derivative) competent cells were transformed with either WT pGEX4T-1 ArfGAP1 or a double mutant pGEX4T-1 ArfGAP1 plasmid and plated on LB agar plates containing ampicillin. Plates were incubated overnight at 37°C. The following day, cells were scraped into a 1 L LB culture containing 100 µg/ml ampicillin and shaken at 220 rpm and 37°C to an OD<sub>600</sub> of approximately 0.6 abs units. The cultures were induced with Isopropyl-β-d-1-thiogalactopyranoside (IPTG) to a final concentration of 400 µM and shaken for 4 h at room temperature. Cells were pelleted by centrifugation at 3,000× g for 15 min at 4°C. Resulting pellets were resuspended in 30 ml of a buffer containing 50 mM Tris–HCl pH 7.5, 150 mM NaCl, 1 mM dithiothreitol (DTT), and 1 mM phenylmethylsulfonyl fluoride (PMSF). The resuspended cells were subjected to lysis via sonication on ice for a total process time of 2 min and 30 s in 30-s pulse intervals with 60 s of rest in between. The resulting lysate was pelleted by centrifugation at 30,000× g for 30 min at 4°C. The soluble fraction was taken and mixed with approximately 500 µl of packed Glutathione (GST) beads pre-washed once with dH<sub>2</sub>O and once with the resuspension buffer. The mixture was rocked at 4°C for 30 min. The beads were pelleted by centrifugation at 800× g for 5 min. The supernatant was aspirated, and pelleted beads were resuspended in 50 ml of resuspension buffer for washing. The mixture was rocked at 4°C for 15 min. The

beads were subsequently pelleted as before, and the wash buffer was removed. Beads were finally resuspended in 5 ml of an elution buffer containing 50 mM Tris-HCl pH 7.5, 150 mM NaCl, 1 mM DTT, and 12 mM reduced glutathione. The mixture was loaded onto a column, and the elution was collected. Resulting protein was concentrated using a 10 kDa centrifugal concentrator, flash-frozen in liquid nitrogen, and stored at  $-80^{\circ}\text{C}$  for future use.

For GST binding assays, HEK293A cells were plated in 3 of 15 cm plates. 5 mg of FLAG-tagged mTOR or Flag-tagged Raptor plasmid was transiently overexpressed per plate for 24 h. Transfected cells or HEK293A cells stably overexpressing FLAG-tagged mLST8 were then collected and immunoprecipitated with FLAG beads (Sigma, #A2220) overnight using CHAPS lysis buffer. Beads were then washed once in CHAPS lysis buffer and incubated for 1 h with 1 mg of GST-EV, GST-ArfGAP1 wild type, or GST-ArfGAP1 L207/V279D mutant, then washed twice more in CHAPS lysis buffer, and Western blot analysis was performed.

### Western blot

Cells were rinsed with PBS and lysed with Laemmli sample buffer (50 mM Tris pH 6.8, 2% SDS, 0.025% Bromophenol Blue, 10% glycerol, 5% BME) and boiled for 5–10 min before separation by 10–15% SDS-PAGE and transfer to polyvinylidene difluoride membranes (#162-0177 from Bio-Rad). Blots were then blocked in 5% milk for 1 h, probed with primary antibodies and horseradish peroxidase (HRP) conjugated secondary antibodies, and developed with SuperSignal<sup>TM</sup> West Dura Substrate (#34075 from Thermo Fisher Scientific).

### Immunofluorescence microscopy

HEK293A cells were seeded in 24-well plates on coverslips (VWR #89015-725) 1 day prior to experimentation. Coverslips were pretreated with 5  $\mu\text{g}/\text{ml}$  of fibronectin (#F4759 from Sigma) at  $37^{\circ}\text{C}$  for 1 h, with a quick phosphate-buffered saline (PBS) wash prior to cell seeding. Cells were transfected with HA-tagged ArfGAP1 for 24 h. For immunofluorescence staining, cells were first briefly washed with PBS and fixed with 4% paraformaldehyde (#15710 from Electron Microscopy Sciences) in PBS for 20 min, followed by washing with PBS three times for 5 min each. Cells were then permeabilized with 0.2% Triton X-100 in PBS for 10 min and blocked in 2% BSA in TBS-Tween (TBST) for 1 h, followed by washing with TBST three times for 5 min each. Cells were incubated for 1 h with primary antibodies (diluted in PBS) and washed with PBS three times for 5 min each. Cells were incubated for 1 h with secondary antibodies or primary antibody conjugated with fluorescent probe (diluted in PBS), followed by PBS (twice for 5 min each) and double distilled water wash (twice for 5 min each). Coverslips were then mounted onto microscope slides (#12-550-15 from Thermo Fisher Scientific) using ProLong Gold Antifade Reagent with DAPI (#P36931 from Thermo Fisher Scientific). Images were captured with a Zeiss LSM 800 confocal microscope. Images depicted in figures were exported from Zeiss ZEN imaging software. Individual channels were pseudo-colored using ImageJ prior to assembling figures. Co-localization analysis was performed using ImageJ. For Fig 4A and B, the co-localization of mTOR and LAMP2 was analyzed using the Squash segmentation and analysis algorithm in ImageJ (Rizk et al, 2014).

### Lifetime imaging and fluctuation analysis of Raptor-ArfGAP1 interaction

Fluorescence lifetime imaging microscopy (FLIM) and raster imaging correlation spectroscopy (RICS) data were collected using an Alba fluorescence correlation spectrometer (ISS, Champaign, IL), connected to a Nikon TE2000-U inverted microscope (Nikon, Melville, NY) with x-y scanning mirror and a PlanApo VC  $60 \times 1.2$  NA water objective as previously described (Goo et al, 2018; Nguyen et al, 2019). Two-photon excitation was provided by a Chameleon Ultra (Coherent, Santa Clara, CA) tuned to 920 nm for FLIM data collection, while 1,000 nm was used for RICS experiments to obtain optimal excitation of both fluorophores (laser power  $> 1$  mW at plane of excitation). Cells were imaged using a temperature and humidity-controlled stage at  $37^{\circ}\text{C}$  with an objective wrap heater (Tokai Hit, Fujinomiya, Shizuoka, Japan) to mimic the environment of the incubator and minimize temperature drift.

FLIM measurements were obtained with an ISS A320 FastFLIM box with photomultiplier detector joined to the Ti:Sapphire laser that created 80 fs pulses at a repetition rate of 80 MHz (H7422P-40, Hamamatsu, Hamamatsu City, Japan). A 680 nm short-pass filter (FF01-680; Semrock, Rochester, NY) and dichroic mirror (500/40 $\times$ , 535lpxr, 645/65 m Chroma, Bellows Falls, VT) was used to spectrally filter the emission of the fluorophores with separate photomultiplier tubes. Fluorescein, in 0.1 M NaOH, and purified EGFP in a filtered 5% BSA/PBS solution was used for standardizing lifetimes (4.0 and 2.95 ns, respectively). Using this method, the fluorescence lifetimes associated with each pixel are analyzed using the phasor plot data (Digman et al, 2008). If energy transfer occurs, the GFP pixels will move into the universal circle due to a shortening of the donor lifetime. During co-transfection experiments, a control plasmid (RFP1) was co-transfected with the Raptor-GFP to establish that the interaction was not due to the fluorescent protein interacting with our protein of interest.

RICS was also used to examine the potential alterations in protein dynamics (Digman et al, 2005; Digman et al, 2008). In short, we selected 12.8  $\mu\text{m}$  (50 nm/pixel) regions of interest (ROI) for each cell that encompassed the majority of the cytosol while attempting to avoid the cell nucleus and plasma membrane. Each cell analyzed consisted of a frame size of  $256 \times 256$  pixels, a pixel sampling time of 12.5  $\mu\text{s}$ , and measurement of 100 frames (approximately 1 min of sampling time per cell). Beam waist ( $\omega_0$ ) calibration was performed daily before each experiment by utilizing the GFP solution standard and was consistently recorded around 0.35–0.4  $\mu\text{m}$ . SimFCS (obtained from the Laboratory for Fluorescence Dynamics) was used to analyze all data obtained from the above-described experiments. Descriptive details on analysis via these software packages have been previously described (Digman et al, 2008; Rossow et al, 2010).

### RNA interference

Dicer-substrate short interfering RNAs (DsiRNAs) against *ARFGAP1* were obtained from IDT (#hs. Ri.ARFGAP1.13). DsiRNAs were delivered into Mia Paca-2 cells using Lullaby transfection reagent (#LL71000 from OZ Biosciences) according to manufacturer's instructions. To achieve optimal knockdown efficiency, cells were transfected again 48 h after first transfection. 24 h after the second

transfection, cells were harvested and analyzed via Western blot analysis, or split for cell proliferation assays.

For RagA/B KO HEK293A cells and Mia Paca-2 cells, *ARFGAP1* was also stably knocked down by short hairpin RNAs (shRNAs). pLKO lentiviral vectors containing *ARFGAP1* shRNAs (from Sigma) were transfected into HEK293A cells together with packaging plasmids pMD2.G and pSPAX2, and the produced recombinant lentiviruses were collected from the medium 48 h post-transfection, followed by 0.45  $\mu\text{m}$  filtering. RagA/B KO HEK293A or Mia Paca-2 cells were then infected with the recombinant lentiviruses with 8  $\mu\text{g}/\text{ml}$  polybrene (TR-1003-G from Millipore), followed by selection of infected cells using puromycin (5  $\mu\text{g}/\text{ml}$ ; #ant-pr-1 from InvivoGen).

Sequences of these DsiRNAs and shRNAs are shown below:  
siArfGAP1-1 duplex:

siArfGAP1-1 duplex:

rArUrUrUrGrArCrCrCrArArGrArArUrCrArGrCrArArCrUGC  
rGrCrArGrUrUrGrCrUrGrArUrUrCrUrUrGrGrUrCrArArArUrGrG

siArfGAP1-2 duplex:

rCrArGrUrUrCrArCrUrArCrGrCrArGrUrArUrCrUrCrUrGGG  
rCrCrArGrArGrArUrArCrUrGrCrGrUrArGrUrGrArArCrUrGrCrC

siArfGAP1-3 duplex:

rGrCrArGrUrUrCrArCrUrArCrGrCrArGrUrArUrCrUrCrUGC  
rCrArGrArGrArUrArCrUrGrCrGrUrArGrUrGrArArCrUrGrCrCrG

shArfGAP1-1 (TRCN0000047322):  
CCGGGTGCAGGATGAGAACAACGTTCTCGAGAACGTTGTTCTCATC  
CTGCACTTTTTG

shArfGAP1-2 (TRCN0000293964):

CCGGCCAGTTCACGCAGTATCCTCGAGGATACTGCGTAGTGA  
ACTGGCTTTTTG

#### RNA extraction, reverse transcription, and real-time PCR

Cells were washed with cold PBS and subjected to RNA extraction using a RNeasy Plus mini kit (#74104 from Qiagen). RNA samples (1  $\mu\text{g}$ ) were reverse-transcribed to complementary DNA using iScript Reverse Transcription Supermix (#1708841 from Bio-Rad). Complementary DNA was then 10 $\times$  diluted and used for quantification (with GAPDH gene as an internal control) by real-time PCR, which was performed using iTaq Universal SYBR Green Supermix (#172-5121 from Bio-Rad) and the CFX96 real-time PCR system (Bio-Rad) using predesigned primers from Sigma Aldrich.

#### Cell proliferation assays

Cells were seeded in 6-well plates or 12-well plates in complete media. Cell number was counted at indicated time points using an automated cell counter (Bio-Rad #TC-20). 3–6 replicated wells were counted per group.

Specifically, MIA Paca-2 cells were transfected with HA-ArfGAP1 or HA-RFP1 as a control in 12-well plates for 4 days prior to cell counting. 6 replicated wells were counted per group. MIA Paca-2 cells with ArfGAP1 stably knocked down, and control cells were seeded in 6-well plates at  $2 \times 10^4$  cells/well and counted at the indicated timepoint. 6 replicated wells were counted per group. After 24 h, cells were treated with either DMSO or 250 nM Torin1 and again after 48 h and counted on day 2. MIA Paca-2 cells were

doubly transfected with siRNAs against *ARFGAP1* and seeded in 12-well plates at  $10^5$  cells/well and counted at 24, 48, and 72 h. 4 replicated wells were counted per group. Mouse PaCa cells stably overexpressing ArfGAP1 or control cells were seeded in 12-well plates at  $3 \times 10^4$  cells/well and counted at 24, 48, and 72 h. 6 replicated wells were counted per group. HEK293A cells were transfected with HA-ArfGAP1 or HA-RFP1 as a control in 6-well plates, and cells were counted at 48 and 96 h. Three replicated wells were counted per group.

#### Cell size

Wild-type or ArfGAP1 stable knockdown Mia Paca-2 cells were seeded into 6 cm plates. For ArfGAP1 overexpression, HEK293A cells were seeded into 6 cm plates and transfected with 4  $\mu\text{g}$  of HA-ArfGAP1 or HA-RFP1 as a control for 48 h. Cells were harvested by trypsinization and resuspended in 1 ml PBS, diluted 1:50 with counting solution (isoton, Beckman Coulter), and cell diameters were determined using a particle size counter (Coulter Z2, Beckman Coulter) with Coulter Z2 AccuComp software. Four replicates were tested for each condition.

#### Generation of *ARFGAP1* knockout cells using CRISPR/Cas9 genome editing

The 20 nucleotide guide sequences targeting human *ARFGAP1* were designed using a CRISPR design tool (Hsu *et al*, 2013) and cloned into a bicistronic expression vector (pX459) containing human codon-optimized Cas9 and the RNA components (Ran *et al*, 2013) (Addgene #62988). The guide sequences targeting exon 4 of human *ARFGAP1* are shown below.

Guide1: 5'- AGGAGGATTACGATCCTTGC –3'

Guide2: 5' -CAGAGCCGCGCCCTCTTA –3'

The single guide RNAs (sgRNAs) in the pX459 vector (1  $\mu\text{g}$ ) were transfected into RagA/B KO HEK293A cells using PolyJet<sup>TM</sup> DNA *In Vitro* Transfection Reagent according to manufacturer's instructions. 24 h post-transfection, cells were treated with 5  $\mu\text{g}/\text{ml}$  puromycin (#ant-pr-1 from InvivoGen) for another 24 h until all the untransfected control cells died. Cells were allowed to recover for couple days prior to single cell sorting into 96-well plate format with DMEM containing 30% FBS by FACs (UT Southwestern; Flow Cytometry Core). Single clones were expanded and screened for ArfGAP1 by protein immunoblotting. Genomic DNA (gDNA) was purified from clones using the Quick-gDNA prep kit (#D3007 Zymo Research), and the region surrounding the guide RNA targeting region was amplified with Q5 high-fidelity DNA polymerase (#M0492L from New England Biolabs) using the following primers (linkers containing *EcoRI* and *XhoI* restriction sites are underlined):

Forward, CCGGAATTCctgcttctgtgtctaatctctag;

Reverse, CCGCTCGAGaataaacggtcacagctgcttc.

PCR products were purified using the DNA Clean and Concentrator Kit (#D4006 from Zymo Research) and cloned into pBluescript II KS+. To determine the indels of individual alleles, at least 10 bacterial colonies were expanded and the plasmid DNA purified and sequenced.

## Mass spectrometry analysis

For mass spectrometry identification of Raptor-interacting proteins, Flag-Raptor was immunoprecipitated with the FLAG M2 affinity gel (#A2220 from Sigma) from RagA/B KO HEK293A cells stably expressing Flag-tagged Raptor. Four 15 cm plates were collected and cells lysed in 4 ml of lysis buffer. After centrifugation, cell lysates were incubated with 50  $\mu$ l anti-Flag M2-Agarose slurry (which was pre-blocked with BSA and washed with lysis buffer before use) for 2 h. After five times of wash with lysis buffer, immunoprecipitated proteins were eluted with 40  $\mu$ l of 3XFlag peptide (#F3290 from Sigma) for 1 h. Elution was repeated and eluted proteins were pooled, boiled in SDS loading buffer, and briefly run on 4–15% precast SDS-PAGE gels (#4561094 from Bio-Rad). Full samples were excised from the gel and analyzed by mass spectrometry. Samples were reduced with DTT and alkylated with iodoacetamide, and then digested with trypsin (MS grade) overnight at 37°C. Tryptic peptides were de-salted via solid-phase extraction (SPE) prior to mass spectrometry analysis. LC-MS/MS experiments were performed on a Thermo Scientific EASY-nLC liquid chromatography system coupled to a Thermo Scientific Orbitrap Fusion Lumos mass spectrometer. To generate MS/MS spectra, MS1 spectra were first acquired in the Orbitrap mass analyzer (resolution 120,000). Peptide precursor ions were then isolated and fragmented using high-energy collision-induced dissociation (HCD). The resulting MS/MS fragmentation spectra were acquired in the ion trap. MS/MS spectral data were searched using Proteome Discoverer 2.1 software (Thermo Scientific) against entries included in the Human Uniprot protein database. Carbamidomethylation of cysteine residues (+57.021 Da) was searched as a static modification and oxidation of methionine (+15.995 Da) and acetylation of peptide N-termini (+42.011 Da) were searched as dynamic modifications. Precursor and product ion mass tolerances of 15 ppm and 0.6 Da were used, respectively. Peptide spectral matches were adjusted to a 1% false discovery rate (FDR), and additionally, proteins were filtered to a 5% FDR. The experiment was performed one time, and there were 245 protein hits. ArfGAP1 was selected to further explore, and we validated ArfGAP1 as a mTORC1-interacting protein through immunoprecipitation experiments from cells.

## Statistical analysis

Statistical analyses were conducted using Prism 7 (GraphPad) and R. Two-tailed Student's *t*-tests were used for comparison between two groups. Fisher's exact test (two-sided) was used to analyze the correlation between HA-ArfGAP1 overexpression and phosphorylation of S6 in confocal images. For survival analysis of ArfGAP1 expression, RNA-seq data and clinical information of TCGA pancreatic cancer cohort were obtained from cBioPortal (<http://www.cbioportal.org/public-portal/>). ARFGAP1 mRNA levels were dichotomized to high and low according to the median expression. Overall survival (OS) was defined as the elapsed time between diagnosis and death or the last follow-up. Survival curves were plotted by the Kaplan–Meier method and compared by the log-rank test. Hazard ratio (HR) and 95% confidence intervals (CI) were also estimated.  $P < 0.05$  were considered as statistically significant. Figures were plotted using Prism 7 (GraphPad).

## Data availability

The mass spectrometry data from this study are available at PRIDE with the accession number PXD024603 (<https://www.ebi.ac.uk/pride/archive/projects/PXD024603>).

**Expanded View** for this article is available online.

## Acknowledgements

We thank Dr. Joseph Albanesi for valuable suggestions. We are grateful to all members of the Jewell laboratory for insightful discussions. We thank Gina Park for help with the GST protein purification. We thank Huyen Nguyen, Teresa Yoon, and Greg Urquhart for technical help. We thank Krzysztof Gonciarz from the MOSAIC group at Max Planck Institute of Molecular Cell Biology and Genetics (MPI-CBG) for technical help for the use of the Squassh segmentation algorithm. This work was supported by grants from Cancer Prevention Research Institute of Texas (CPRIT) Scholar Recruitment of First-Time, Tenure-Track Faculty Member (RR150032), Cancer Prevention Research Institute of Texas (CPRIT) High-Impact/High-Risk Research Award (RP160713), The Welch Foundation (I-1927-20170325 & I-1927-20200401), 2017 UT Southwestern President's Research Council Distinguished Researcher Award, American Cancer Society Research Scholar Grant (133894-RSG-19-162-01-TBE), National Institutes of Health (R01GM129097-01) to J.L.J., and (P20 GM113134/GM/NIGMS and R01 GM123048/GM/NIGMS) to N.J.

## Author contributions

Author contributions: DM and JIJ designed the experiments. DM, QY, CHM, BCP, AC, and M-HJ conducted the experiments. DM and T-SH analyzed confocal images. JZ conducted mass spectrometry analysis. NGJ performed the lifetime imaging and fluctuation analysis. DM and JIJ wrote the manuscript with input from all the authors.

## Conflict of interest

The authors declare that they have no conflict of interest.

## References

- Abu-Remaileh M, Wyant GA, Kim C, Laqtom NN, Abbasi M, Chan SH, Freinkman E, Sabatini DM (2017) Lysosomal metabolomics reveals V-ATPase- and mTOR-dependent regulation of amino acid efflux from lysosomes. *Science* 358: 807–813
- Bai M, Gad H, Turacchio G, Cocucci E, Yang J-S, Li J, Beznoussenko GV, Nie Z, Luo R, Fu L *et al* (2011) ARFGAP1 promotes AP-2-dependent endocytosis. *Nat Cell Biol* 13: 559–567
- Bar-Peled L, Chantranupong L, Cherniack AD, Chen WW, Ottina KA, Grabiner BC, Spear ED, Carter SL, Meyerson M, Sabatini DM (2013) A Tumor suppressor complex with GAP activity for the Rag GTPases that signal amino acid sufficiency to mTORC1. *Science* 340: 1100–1106
- Bar-Peled L, Schweitzer LD, Zoncu R, Sabatini DM (2012) Ragulator is a GEF for the rag GTPases that signal amino acid levels to mTORC1. *Cell* 150: 1196–1208
- Bauchart-Thevret C, Cui L, Wu G, Burrin DG (2010) Arginine-induced stimulation of protein synthesis and survival in IPEC-J2 cells is mediated by mTOR but not nitric oxide. *Am J Physiol Endocrinol Metab* 299: E899–909
- Ben-Sahra I, Manning BD (2017) mTORC1 signaling and the metabolic control of cell growth. *Curr Opin Cell Biol* 45: 72–82

- Betz C, Hall MN (2013) Where is mTOR and what is it doing there? *J Cell Biol* 203: 563–574
- Bigay J, Casella JF, Drin G, Mesmin B, Antonny B (2005) ArfGAP1 responds to membrane curvature through the folding of a lipid packing sensor motif. *EMBO J* 24: 2244–2253
- Bigay J, Gounon P, Robineau S, Antonny B (2003) Lipid packing sensed by ArfGAP1 couples COPI coat disassembly to membrane bilayer curvature. *Nature* 426: 563–566
- Blenis J (2017) TOR, the Gateway to Cellular Metabolism, Cell Growth, and Disease. *Cell* 171: 10–13
- Bos JL, Rehmann H, Wittinghofer A (2007) GEFs and GAPs: critical elements in the control of small G proteins. *Cell* 129: 865–877
- Burnett PE, Barrow RK, Cohen NA, Snyder SH, Sabatini DM (1998) RAFT1 phosphorylation of the translational regulators p70 S6 kinase and 4E-BP1. *Proc Natl Acad Sci USA* 95: 1432–1437
- Chantranupong L, Scaria SM, Saxton RA, Gygi MP, Shen K, Wyant GA, Wang T, Harper JW, Gygi SP, Sabatini DM (2016) The CASTOR proteins are arginine sensors for the mTORC1 pathway. *Cell* 165: 153–164
- Cukierman E, Huber I, Rotman M, Cassel D (1995) The ARF1 GTPase-activating protein: zinc finger motif and Golgi complex localization. *Science* 270: 1999–2002
- Digman MA, Brown CM, Sengupta P, Wiseman PW, Horwitz AR, Gratton E (2005) Measuring fast dynamics in solutions and cells with a laser scanning microscope. *Biophys J* 89: 1317–1327
- Digman MA, Caiolfa VR, Zamai M, Gratton E (2008) The phasor approach to fluorescence lifetime imaging analysis. *Biophys J* 94: L14–16
- Donaldson JG, Jackson CL (2011) ARF family G proteins and their regulators: roles in membrane transport, development and disease. *Nat Rev Mol Cell Biol* 12: 362–375
- Duran RV, Hall MN (2012) Regulation of TOR by small GTPases. *EMBO Rep* 13: 121–128
- Efeyan A, Zoncu R, Sabatini DM (2012) Amino acids and mTORC1: from lysosomes to disease. *Trends Mol Med* 18: 524–533
- Faini M, Beck R, Wieland FT, Briggs JA (2013) Vesicle coats: structure, function, and general principles of assembly. *Trends Cell Biol* 23: 279–288
- Fingar DC, Richardson CJ, Tee AR, Cheatham L, Tsou C, Blenis J (2004) mTOR controls cell cycle progression through its cell growth effectors S6K1 and 4E-BP1/eukaryotic translation initiation factor 4E. *Mol Cell Biol* 24: 200–216
- Fingar DC, Salama S, Tsou C, Harlow E, Blenis J (2002) Mammalian cell size is controlled by mTOR and its downstream targets S6K1 and 4EBP1/eIF4E. *Genes Dev* 16: 1472–1487
- Flinn RJ, Yan Y, Goswami S, Parker PJ, Backer JM (2010) The late endosome is essential for mTORC1 signaling. *Mol Biol Cell* 21: 833–841
- Gonzalez A, Hall MN (2017) Nutrient sensing and TOR signaling in yeast and mammals. *EMBO J* 36: 397–408
- Goo B, Sanstrum BJ, Holden DZY, Yu Y, James NG (2018) Arc/Arg3.1 has an activity-regulated interaction with PICK1 that results in altered spatial dynamics. *Sci Rep* 8: 14675
- Gu X, Orozco JM, Saxton RA, Condon KJ, Liu GY, Krawczyk PA, Scaria SM, Harper JW, Gygi SP, Sabatini DM (2017) SAMTOR is an S-adenosylmethionine sensor for the mTORC1 pathway. *Science* 358: 813–818
- Hara K, Yonezawa K, Weng QP, Kozlowski MT, Belham C, Avruch J (1998) Amino acid sufficiency and mTOR regulate p70 S6 kinase and eIF-4E BP1 through a common effector mechanism. *J Biol Chem* 273: 14484–14494
- Hsu PD, Scott DA, Weinstein JA, Ran FA, Konermann S, Agarwala V, Li Y, Fine EJ, Wu X, Shalem O et al (2013) DNA targeting specificity of RNA-guided Cas9 nucleases. *Nature Biotechnol* 31: 827–832.
- Inoki K, Li Y, Xu T, Guan KL (2003) Rheb GTPase is a direct target of TSC2 GAP activity and regulates mTOR signaling. *Genes Dev* 17: 1829–1834
- Itzen A, Goody RS (2011) GTPases involved in vesicular trafficking: structures and mechanisms. *Semin Cell Dev Biol* 22: 48–56
- Jackson CL, Bouvet S (2014) Arfs at a glance. *J Cell Sci* 127: 4103–4109
- Jewell JL, Kim YC, Russell RC, Yu FX, Park HW, Plouffe SW, Tagliabracchi VS, Guan KL (2015) Metabolism. Differential regulation of mTORC1 by leucine and glutamine. *Science* 347: 194–198
- Jewell JL, Russell RC, Guan KL (2013) Amino acid signalling upstream of mTOR. *Nat Rev Mol Cell Biol* 14: 133–139
- Kim E, Goraksha-Hicks P, Li L, Neufeld TP, Guan KL (2008) Regulation of TORC1 by Rag GTPases in nutrient response. *Nat Cell Biol* 10: 935–945
- Kim J, Kundu M, Viollet B, Guan KL (2011) AMPK and mTOR regulate autophagy through direct phosphorylation of Ulk1. *Nat Cell Biol* 13: 132–141
- Lawrence RE, Zoncu R (2019) The lysosome as a cellular centre for signalling, metabolism and quality control. *Nat Cell Biol* 21: 133–142
- Lee SY, Yang JS, Hong W, Premont RT, Hsu VW (2005) ARFGAP1 plays a central role in coupling COPI cargo sorting with vesicle formation. *J Cell Biol* 168: 281–290
- Li L, Kim E, Yuan H, Inoki K, Goraksha-Hicks P, Schiesher RL, Neufeld TP, Guan KL (2010) Regulation of mTORC1 by the Rab and Arf GTPases. *J Biol Chem* 285: 19705–19709
- Liu GY, Sabatini DM (2020) mTOR at the nexus of nutrition, growth, ageing and disease. *Nat Rev Mol Cell Biol* 21: 183–203
- Maehama T, Tanaka M, Nishina H, Murakami M, Kanaho Y, Hanada K (2008) RalA functions as an indispensable signal mediator for the nutrient-sensing system. *J Biol Chem* 283: 35053–35059
- Makler V, Cukierman E, Rotman M, Admon A, Cassel D (1995) ADP-ribosylation factor-directed GTPase-activating protein. Purification and partial characterization. *J Biol Chem* 270: 5232–5237
- Manifava M, Smith M, Rotondo S, Walker S, Niewczas I, Zoncu R, Clark J, Ktistakis NT (2016) Dynamics of mTORC1 activation in response to amino acids. *Elife* 5: e19960
- Meng D, Frank AR, Jewell JL (2018) mTOR signaling in stem and progenitor cells. *Development* 145: dev152595
- Meng D, Yang Q, Wang H, Melick CH, Navlani R, Frank AR, Jewell JL (2020) Glutamine and asparagine activate mTORC1 independently of Rag GTPases. *J Biol Chem* 295: 2890–2899
- Menon S, Dibble CC, Talbott G, Hoxhaj G, Valvezan AJ, Takahashi H, Cantley LC, Manning BD (2014) Spatial control of the TSC complex integrates insulin and nutrient regulation of mTORC1 at the lysosome. *Cell* 156: 771–785
- Mesmin B, Drin G, Levi S, Rawet M, Cassel D, Bigay J, Antonny B (2007) Two lipid-packing sensor motifs contribute to the sensitivity of ArfGAP1 to membrane curvature. *Biochemistry* 46: 1779–1790
- Mossmann D, Park S, Hall MN (2018) mTOR signalling and cellular metabolism are mutual determinants in cancer. *Nat Rev Cancer* 18: 744–757
- Nguyen H, Ward WS, James NG (2019) Spatial and temporal resolution of mTORC4 fluorescent variants reveals structural requirements for achieving higher order self-association and pronuclei entry. *Methods Appl Fluoresc* 7: 35002
- Nguyen TP, Frank AR, Jewell JL (2017) Amino acid and small GTPase regulation of mTORC1. *Cell Logist* 7: e1378794
- Ran FA, Hsu PD, Wright J, Agarwala V, Scott DA, Zhang F (2013) Genome engineering using the CRISPR-Cas9 system. *Nat Protoc* 8: 2281–2308
- Rawet M, Levi-Tal S, Szafer-Glusman E, Parnis A, Cassel D (2010) ArfGAP1 interacts with coat proteins through tryptophan-based motifs. *Biochem Biophys Res Commun* 394: 553–557

- Rizk A, Paul G, Incardona P, Bugarski M, Mansouri M, Niemann A, Ziegler U, Berger P, Sbalzarini IF (2014) Segmentation and quantification of subcellular structures in fluorescence microscopy images using Squash. *Nat Protoc* 9: 586–596
- Rodriguez-Fernandez IA, Dell'Angelica EC (2015) Identification of Atg2 and ArfGAP1 as candidate genetic modifiers of the eye pigmentation phenotype of adaptor protein-3 (AP-3) mutants in *Drosophila melanogaster*. *PLoS One* 10: e0143026
- Rossow MJ, Sasaki JM, Digman MA, Gratton E (2010) Raster image correlation spectroscopy in live cells. *Nat Protoc* 5: 1761–1774
- Saci A, Cantley LC, Carpenter CL (2011) Rac1 regulates the activity of mTORC1 and mTORC2 and controls cellular size. *Mol Cell* 42: 50–61
- Sancak Y, Bar-Peled L, Zoncu R, Markhard AL, Nada S, Sabatini DM (2010) Ragulator-Rag complex targets mTORC1 to the lysosomal surface and is necessary for its activation by amino acids. *Cell* 141: 290–303
- Sancak Y, Peterson TR, Shaul YD, Lindquist RA, Thoreen CC, Bar-Peled L, Sabatini DM (2008) The Rag GTPases bind raptor and mediate amino acid signaling to mTORC1. *Science* 320: 1496–1501
- Sanger A, Hirst J, Davies AK, Robinson MS (2019) Adaptor protein complexes and disease at a glance. *J Cell Sci* 132: jcs222992
- Sanjana NE, Shalem O, Zhang F (2014) Improved vectors and genome-wide libraries for CRISPR screening. *Nat Methods* 11: 783–784
- Soliman GA, Acosta-Jaquez HA, Dunlop EA, Ekim B, Maj NE, Tee AR, Fingar DC (2010) mTOR Ser-2481 autophosphorylation monitors mTORC-specific catalytic activity and clarifies rapamycin mechanism of action. *J Biol Chem* 285: 7866–7879
- Spang A, Shiba Y, Randazzo PA (2010) Arf GAPs: gatekeepers of vesicle generation. *FEBS Lett* 584: 2646–2651
- Stafa K, Trancikova A, Webber PJ, Glauser L, West AB, Moore DJ (2012) GTPase activity and neuronal toxicity of Parkinson's disease-associated LRRK2 is regulated by ArfGAP1. *PLoS Genet* 8: e1002526
- Szafer E, Pick E, Rotman M, Zuck S, Huber I, Cassel D (2000) Role of coatomer and phospholipids in GTPase-activating protein-dependent hydrolysis of GTP by ADP-ribosylation factor-1. *J Biol Chem* 275: 23615–23619
- Tee AR, Manning BD, Roux PP, Cantley LC, Blenis J (2003) Tuberous sclerosis complex gene products, Tuberin and Hamartin, control mTOR signaling by acting as a GTPase-activating protein complex toward Rheb. *Curr Biol* 13: 1259–1268
- Terenzio M, Koley S, Samra N, Rishal I, Zhao Q, Sahoo PK, Urisman A, Marvaldi L, Oses-Prieto JA, Forester C et al (2018) Locally translated mTOR controls axonal local translation in nerve injury. *Science* 359: 1416–1421
- Thomas JD, Zhang YJ, Wei YH, Cho JH, Morris LE, Wang HY, Zheng XF (2014) Rab1A is an mTORC1 activator and a colorectal oncogene. *Cancer Cell* 26: 754–769
- Tsun ZY, Bar-Peled L, Chantranupong L, Zoncu R, Wang T, Kim C, Spooner E, Sabatini DM (2013) The folliculin tumor suppressor is a GAP for the RagC/D GTPases that signal amino acid levels to mTORC1. *Mol Cell* 52: 495–505
- Wolfson RL, Chantranupong L, Saxton RA, Shen K, Scaria SM, Cantor JR, Sabatini DM (2016) Sestrin2 is a leucine sensor for the mTORC1 pathway. *Science* 351: 43–48
- Xiong Y, Yuan C, Chen R, Dawson TM, Dawson VL (2012) ArfGAP1 is a GTPase activating protein for LRRK2: reciprocal regulation of ArfGAP1 by LRRK2. *J Neurosci* 32: 3877–3886
- Xu L, Salloum D, Medlin PS, Saqçena M, Yellen P, Perrella B, Foster DA (2011) Phospholipase D mediates nutrient input to mammalian target of rapamycin complex 1 (mTORC1). *J Biol Chem* 286: 25477–25486
- Yang H, Jiang X, Li B, Yang HJ, Miller M, Yang A, Dhar A, Pavletich NP (2017) Mechanisms of mTORC1 activation by RHEB and inhibition by PRAS40. *Nature* 552: 368–373
- Yang JS, Lee SY, Gao M, Bourgoin S, Randazzo PA, Premont RT, Hsu VW (2002) ARFGAP1 promotes the formation of COPI vesicles, suggesting function as a component of the coat. *J Cell Biol* 159: 69–78
- Zhang Y, Gao X, Saucedo LJ, Ru B, Edgar BA, Pan D (2003) Rheb is a direct target of the tuberous sclerosis tumour suppressor proteins. *Nat Cell Biol* 5: 578–581
- Zhu M, Wang XQ (2020) Regulation of mTORC1 by small GTPases in response to nutrients. *J Nutr* 150: 1004–1011
- Zoncu R, Bar-Peled L, Efeyan A, Wang S, Sancak Y, Sabatini DM (2011) mTORC1 senses lysosomal amino acids through an inside-out mechanism that requires the vacuolar H(+)-ATPase. *Science* 334: 678–683



**License:** This is an open access article under the terms of the Creative Commons Attribution-NonCommercial-NoDerivs License, which permits use and distribution in any medium, provided the original work is properly cited, the use is noncommercial and no modifications or adaptations are made.